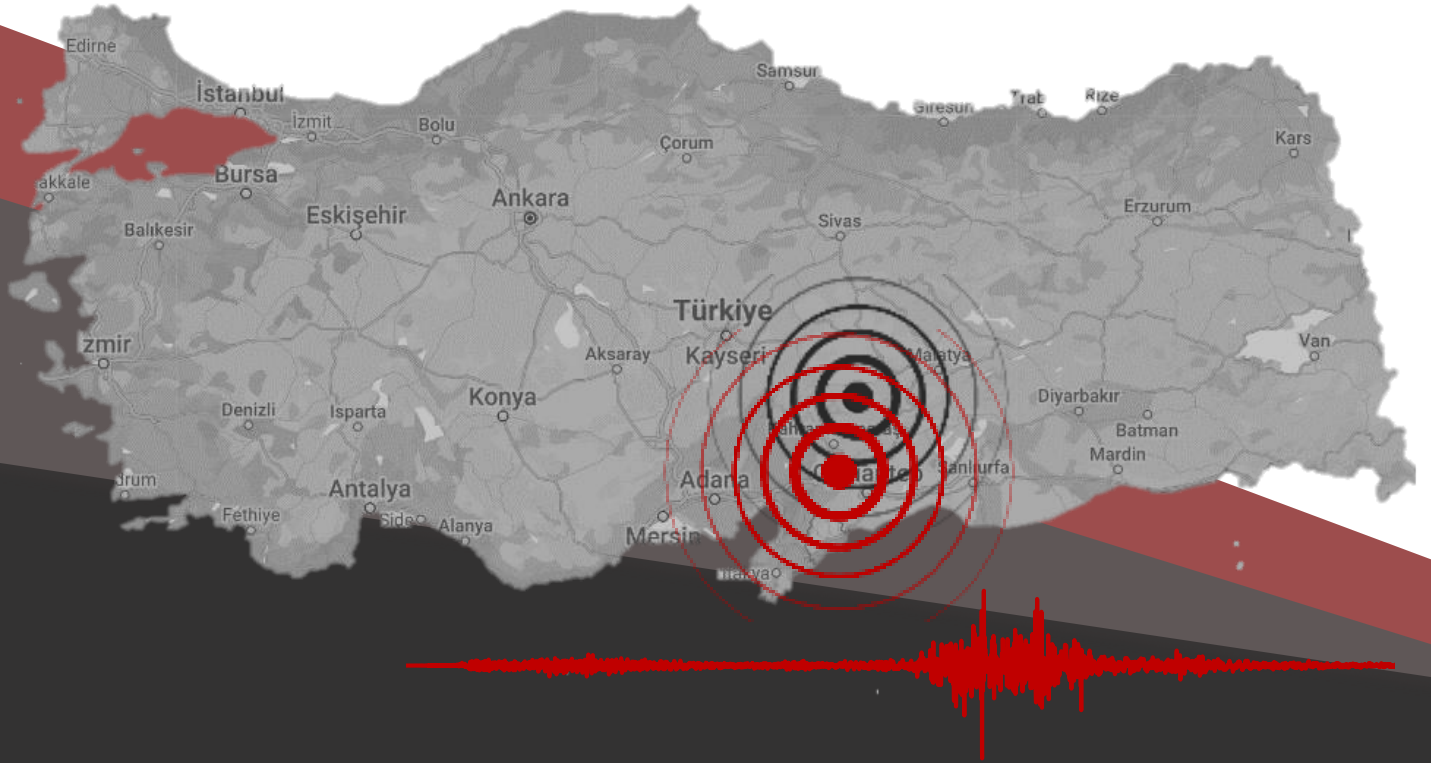




MIDDLE EAST TECHNICAL UNIVERSITY

Preliminary Reconnaissance Report on February 6, 2023, Pazarcık $M_w=7.7$ and Elbistan $M_w=7.6$, Kahramanmaraş-Türkiye Earthquakes



Edited by: Kemal Önder Çetin, Makbule İlgaç, Gizem Can and Elife Çakır

February 20, 2023

REPORT NO: METU/EERC 2023-01

EARTHQUAKE ENGINEERING RESEARCH CENTER





Preface

The February 6, 2023, Kahramanmaraş earthquakes, affecting a total of eleven provinces, deeply affected us all. I write to you today with a heavy heart, as our thoughts and prayers are with our people in the aftermath of the devastating earthquakes that struck the country on February 6. The earthquakes, which measured moment magnitudes 7.7 and 7.6 hit the provinces of Kahramanmaraş, Adıyaman, Hatay, Osmaniye, Gaziantep, Kilis, Şanlıurfa, Diyarbakır, Malatya, Adana, and Elazığ in eastern Türkiye, causing significant damage to buildings and infrastructure and claiming the lives of dozens of our people. Our deepest sympathies go out to the families and loved ones of those who lost their lives or were injured in the earthquakes, and we offer our support and solidarity as they begin the long process of recovery.

As a university community, immediately after the earthquakes, Middle East Technical University faculty members and staff set out to conduct research in the region. Teams from Middle East Technical University (METU), consisting of experts in fields such as civil engineering, geology, architecture, city planning, etc., have initiated to perform preliminary reconnaissance studies in the cities of the region with the collaboration of experts of diverse fields from other university members and institutions. We encourage our faculty, staff, and students to join us in these ongoing efforts and to consider how they can contribute their skills, expertise, and resources to help those affected by the earthquakes.

At times like these, it is important to remember the strength and resilience of the human spirit, and the power of individuals and communities to come together. We are confident that the people of the region will overcome this tragedy, and we stand with them in their efforts to rebuild and recover.

Sincerely,

Prof. Dr. Mustafa Verşan Kök

President, Middle East Technical University



CHAPTERS

CHAPTER 1 Introduction

By:

Kemal Önder Çetin, Ahmet Yakut, Makbule Ilgaç, A. Arda Özacar, Gizem Can, Elife Çakır

CHAPTER 2 Regional Tectonics and Seismic Source

By:

A. Arda Özacar, Bora Uzel, Erdin Bozkurt, Taylan Sançar, Eyüp Sopacı, Nuretdin Kaymakçı, Bora Rojay, Zeynep Gülerce, Cem Kıncal, Laura Gregory

CHAPTER 3 Preliminary Analysis of Strong Ground Motion Characteristics

By:

Zeynep Gülerce, Ayşegül Askan, Özkan Kale, Abdullah Sandıkkaya, Nihat Sinan Işık, Okan İlhan, Gizem Can, Makbule Ilgaç, A. Arda Özacar, Eyüp Sopacı, Kemal Önder Çetin, Burak Akbaş, Abdullah Altındal, Mehmet Fırat Aydın, Baran Güryuva, Onur Kanun, Kubilay Albayrak, Gamze Muratoğlu, Oguz Salih Okçu, Abdullah İçen

CHAPTER 4 Geotechnical Findings and the Performance of Geo-Structures

By:

Kemal Önder Çetin, Candan Gökçeoğlu, Robb Eric Shedwick Moss, Makbule Ilgaç, Gizem Can, Elife Çakır, Bilal Umut Aydın, Arda Şahin, Mehmet Türkezer, Berkan Söylemez, Soner Ocak, Hayri Güzel

CHAPTER 5 Performance of Residential Structures

By:

Barış Binici, Ahmet Yakut, Erdem Canbay, İsmail Ozan Demirel, Mevlüt Kahraman, Altuğ Erberik, İsmail Özgür Yaman, Eray Baran, Afşin Canbolat, Koray Kadaş, Orkun Öztaşkın, Selin Aktaş



CHAPTER 6 Performance of Bridges and Tunnels

By:

Alp Caner, Kemal Önder Çetin, Candan Gökçeoğlu

CHAPTER 7 Coastal Structures in the Gulf of İskenderun Bay and Tsunami in the Eastern Mediterranean

By:

Ahmet Cevdet Yalçınler, Gözde Güney Doğan, Işıkhhan Güler, Bilge Karakütük, Furkan Demir, Didem Cambaz, Vassilios Skanavi, Costas Synolakis

CHAPTER 8 Preliminary Reconnaissance Observations on Lifelines After 6 February 2023 Earthquakes in Türkiye

By:

Nejan Huvaj, Volkan Kalpakcı, Şevki Öztürk, Tamer Y. Duman, Eray Baran, Burak Talha Kılıç, Ali Serdar Uysal, Suat Dalkılıç, Emre Dalkılıç, Onur Pekcan

CHAPTER 9 Preliminary Structural Performance Summary of Historic Structures

By:

Ahmet Türer

CHAPTER 10 Emergency Response and Community Impact

By:

Meltem Şenol Balaban, Ali Fırat Çabalar, A. Nuray Karancı, Canay Doğulu, Gözde İkizer, Haldun Akoğlu, Müge Akın, Nil Akdede, Onur Karakayalı, Özlem Özdemir, Sarper Yılmaz, Selin Güzel, Serkan Yılmaz, Sıdıka Tekeli Yeşil, Tolulope Ajobiewe, Yeşim Ünal



Table of Contents

Chapter 1.....	12
Introduction.....	12
1. 1. Introduction.....	13
Chapter 2.....	17
Regional Tectonics and Seismic Source	17
2. 1. Regional Tectonics.....	18
2. 2. Major Earthquake History.....	18
2. 3. Seismic Source.....	18
2. 4. Surface Rupture and Geological Field Observations	19
2. 5. Seismic Gaps and Static Stress Changes.....	21
Chapter 3.....	24
Preliminary Analysis of Strong Ground Motion Characteristics	24
3. 1. Introduction.....	25
3. 2. Information on Recorded Strong Ground Motions at Selected Stations.....	25
3. 3. Spatial Distribution of Peak Ground Parameters from February 6 Earthquakes	28
Chapter 4.....	30
Geotechnical Findings and the Performance of Geo-Structures	30
4. 1. Geotechnical Observations	31
4. 1. 1. Seismic Soil Liquefaction Manifestations	31
4. 1. 2. Residential Building Foundation Performance	35
4. 1. 3. Deep Excavations.....	36
4. 1. 4. Retaining Structures.....	37
4. 1. 5. Rockfalls	38
4. 1. 6. Tunnels.....	39
4. 1. 7. Landslides	40
4. 1. 8. Ground Deformations	41



4. 1. 9. Faulting induced Pipeline breakage	42
Chapter 5.....	43
Performance of Residential Structures.....	43
5. 1. Performance of Buildings	44
5. 1. 1. Performance of RC Buildings Before 2000	45
5. 1. 2. Performance of RC Buildings After 2000.....	46
5. 1. 3. Performance of Precast Buildings.....	47
5. 1. 4. Performance of Non-Structural Elements	48
5. 1. 5. Performance of Masonry Buildings	49
5. 1. 6. Performance of Strengthened Buildings	50
5. 1. 7. Performance of Electrical Substation Buildings	50
Chapter 6.....	52
Performance of Bridges and Tunnels.....	52
6. 1. Bridge and Tunnel Condition Assessment	53
Chapter 7.....	58
Coastal Structures in the Gulf of İskenderun and Tsunami in The Eastern Mediterranean	58
7. 1. Coastal Structures in the Gulf of İskenderun and Tsunami in The Eastern Mediterranean	59
Chapter 8.....	64
Preliminary Reconnaissance Observations on Lifelines After 6 February 2023 Earthquakes in Türkiye ..	64
8. 1. Introduction.....	65
8. 2. Brief Information about the Critical Infrastructure in The Region	65
8. 3. Field Observations on Lifelines	68
Chapter 9.....	74
Preliminary Structural Performance Summary of Historic Structures.....	74
9. 1. Introduction.....	75
9. 2. Visual Inspection of the Historic Structures	75
Chapter 10.....	85



Emergency Response and Community Impact	85
10. 1. Introduction.....	86
10. 2. Emergency Response	86
10. 2. 1. Coordination	86
10. 2. 2. Immediate Rescue and Response	87
10. 2. 3. Infrastructure.....	87
10. 2. 4. Health Services	87
10. 2. 5. Accommodation Response: Emergency and Temporary Shelter	88
10. 2. 6. Psychosocial Support.....	88
10. 3. Community Impact	88
10. 4. Overview of International Media Response.....	88
10. 5. Conclusion	89



List of Figures

Figure 1.1. Map of Türkiye (Google Maps). The epicenter of the February 6, 2023, Kahramanmaraş-Pazarcık ($M_w=7.7$) and Kahramanmaraş-Elbistan ($M_w=7.6$) Earthquakes are shown with white pins.	13
Figure 2.1. Examples Seismotectonic map showing rupture planes and aftershocks (taken from AFAD) along with global moment tensor solutions of recent major earthquakes. Ruptures are numbered in time and arrows indicate the inferred rupture direction of the initial Pazarcık earthquake ($M_w=7.8$) which displays directivity and discontinuous rupture evolution.....	20
Figure 2.2. Photos of 2.4 m road offset near Pazarcık and 6.7 m fence offset along the Sürgü-Çardak fault segment (taken by Erdin Bozkurt and Taylan Sançar respectively).	20
Figure 2.3. Coulomb static stress change on the neighboring fault segments after the recent earthquake sequence. Calculations were made for left-lateral strike-slip faults using finite fault solutions computed by USGS.	21
Figure 3.1. Distribution of the strong motion stations that are located within 200km of the rupture plane for (a) $M_w=7.7$ Kahramanmaraş-Pazarcık and (b) $M_w=7.6$ Elbistan earthquakes.	26
Figure 3.2. Recorded three-component ground accelerations, corresponding Fourier amplitude spectra (FAS), and response spectra (with 5% damping) in comparison with the most recent building code (TBEC, 2019) at selected stations due to Pazarcık ($M_w=7.7$) event	27
Figure 3.3. Spatial distribution of intensity measure of Pazarcık earthquake (a) PGA, (b) PGV	29
Figure 3.4. Spatial distribution of intensity measure of Elbistan earthquake (a) PGA, (b) PGV .	29
Figure 4.1. Seismic soil liquefaction-induced surface manifestation: sand boils in free field conditions: a) Hatay (36.36446° N, 36.28147°E), b) Kumlu / Hatay (36.35628°N, 36.39360°E), c) Fatih District / Gölbaşı / Adıyaman (37.78080°N, 37.62888°E), d) İskenderun / Hatay (36.59323° N, 36.18542°E), e) Emiroğlu / Kahramanmaraş (37.33689°N, 37.04538°E), f) Çay District / İskenderun / Hatay (36.59133°N, 36.17888°E) g) Dörttyol / Hatay (36.81878°N, 37.17770°E) h) Emiroğlu / Kahramanmaraş (37.33722°N, 37.04549°E) i) Gölbaşı / Adıyaman (37.78655°N, 37.63155°E)	32
Figure 4.2. Seismic soil liquefaction induced lateral spreadings in a) Çay District / İskenderun / Hatay (36.59281°N, 36.185977°), b) Özerli District / Dörttyol / Hatay (36.81294°N, 36.18123°E), c) Fatih District / Gölbaşı / Adıyaman (37.78023°N, 37.62858°E), d) İskenderun Port Area / Hatay	



(36.59991°N, 36.19274°E), e) İskenderun Port Area / Hatay (36.59991°N, 36.19274°E), f) İskenderun Port Area / Hatay (36.59991°N, 36.19274°E)..... 33

Figure 4.3. Seismic soil liquefaction-induced induced foundation problems in a) Çay District / İskenderun / Hatay (36.5911°N, 36.1790°E), b) Çay District / İskenderun / Hatay (36.5911°N, 36.1790°E), c) Çay District / İskenderun / Hatay (36.5911°N, 36.1790°E), d) Çay District / İskenderun / Hatay (36.5911°N, 36.1790°E)..... 34

Figure 4.4. Poor foundation performance in a) Çay District / İskenderun / Hatay (36.5911°N, 36.1790°E), b) Hürriyet District / Gölbaşı / Adıyaman (37.778°N 37.628°E), c) Yavuz Selim District / Gölbaşı / Adıyaman (37.788°N, 37.642°E), d) Yavuz Selim District / Gölbaşı / Adıyaman (37.788°N, 37.642°E), e) Yavuz Selim District / Gölbaşı / Adıyaman (37.78827°N 37.64879°E)..... 35

Figure 4.5. Examples of deep excavations in a) Bahçe / Osmaniye (37.18845° N, 36.56326° E), b) Bahçe / Osmaniye (37.18939° N, 36.56402° E), c) Bahçe / Osmaniye (36.17313° N, 36.59912° E), d) Bahçe / Osmaniye (36.17313° N, 36.59912° E)..... 36

Figure 4.6. Some examples of retaining structures in a) Gökçedere/ Gaziantep (37.16439°N, 36.70672°E), b) Gökçedere/ Gaziantep (37.16546° N, 36.69749°E), c) Bahçe/ Osmaniye (37.18853°N, 36.56389°E), d) Bahçe/ Osmaniye (37.18844° N, 36.56476° E) 37

Figure 4.7. Some examples of rockfalls in a) Bahçe / Osmaniye (37.17441°N, 36.65659°E), b) Yolbağı District / Adıyaman (37.81795°N, 37.63311°E), c) Fevzi Paşa District / İslahiye /Gaziantep (37.09899° N, 36.65200 ° E), d) Fevzi Paşa District / İslahiye /Gaziantep (37.09713° N, 36.65170 ° E) 38

Figure 4.8. Bahçe-Nurdağı railway tunnels under construction in Nurdağı/ Gaziantep (37.16989°N, 36.70806°E) 39

Figure 4.9. Some examples of slope stability problems in a) Gölbaşı/ Adıyaman (37.79783°N, 37.66232°E), b) Yolbağı District / Adıyaman (37.81806°N, 37.63297°E), c) Belen / Hatay (36.48363°N, 36.27158°E) 40

Figure 4.10. Observation of surface rupture trace in a) Balkar / Adıyaman (37.73610°N, 37.56842°E), b) Erenler District / İslahiye / Gaziantep (37.03931°N, 36.62868°E), E), c) Yavuz Selim District / Adıyaman (37.79645°N, 37.66021°E), d) Balkar / Adıyaman (37.73492°N, 37.56617°)..... 41



Figure 4.11. Pipeline damages in a) Erenler District / İslahiye / Gaziantep (36.04621°N, 36.62936°E), b) Çay District / İskenderun / Hatay (36.59038°N, 36.17893°E).....	42
Figure 5.1. Building Collapse in Antakya and Kahramanmaraş.....	45
Figure 5.2. Building Collapse in Malatya.....	46
Figure 5.3. Overturning due to soil liquefaction and insufficient joint reinforcement detailing ..	46
Figure 5.4. Heavily damaged new buildings in Adıyaman and İslahiye	47
Figure 5.5. Performance of a tunnel form building	47
Figure 5.6. Overview of precast industrial building connection damage in Kahramanmaraş.....	48
Figure 5.7. Corbel damages in Gaziantep.....	48
Figure 5.8. Infill wall damage examples.....	49
Figure 5.9. Damage in masonry structures	50
Figure 5.10. Performance of the strengthened building in Hatay.....	50
Figure 5.11. PGA distribution and substation locations (Yellow: Strong motion instruments, Blue and Green: Substation Locations).....	51
Figure 6.1. Abutment rotation due to seismic soil liquefaction induced foundation failure.....	54
Figure 6.2. Joint movements.....	54
Figure 6.3. Concrete spalling.....	54
Figure 6.4. Bearing dislocation and movement	55
Figure 6.5. Rail misalignment.....	55
Figure 6.6. Shear key damage.....	56
Figure 6.7. Abutment wall concrete spalling	56
Figure 6.8. Bridge typical have no damage	57
Figure 6.9. Tunnel portal movement and concrete spalling.....	57
Figure 7.1 a) The location of the possible source of small amplitude tsunami and the tide gauge stations, and b) distribution of maximum water elevations computed from the possible source, North of Çevlik	60
Figure 7.2 The comparison of the measured (black) and computed (blue) time histories of water surface fluctuations at four tide gauge stations (first column) and computed time histories near Karataş, Yumurtalık and Çevlik fishery ports, where only eyewitness observations (second column) could be obtained.....	61
Figure 7.3 Coastal Inundation and traces, South of Samandağ-Çevlik Fishery Port.....	62



Figure 7.4 Structural damage at İskenderun Fishery Port.....	62
Figure 8.1 a) Parts of the state highway network in the region (source: State Highway Agency, KGM website, https://www.kgm.gov.tr/SiteCollectionImages/KGMImages/Haritalar/b5.jpg), b) Parts of the state railway network in the region (source: Turkish State Railway Agency website: https://static.tcdd.gov.tr/webfiles/userfiles/files/genel/tcddharita.pdf)	66
Figure 8.2. Areal view of the surface fault rupture and examples of damages caused by the two earthquakes on some of the lifelines: railway line, roads and water distribution network, near Narlı, Kahramanmaraş (Satellite images are provided by Turkish General Directorate of Maps via atlas.harita.gov.tr website)	69
Figure 8.3. Referring to Figure 2 for locations of the photos: offset on the road due to surface fault rupture, railway embankment slope instability, water pipeline repair works and a tilted electric pole can be seen, near Narlı, Kahramanmaraş. (Active fault data is taken from Emre et al. (2013) published by the General Directorate of Mineral Research and Exploration, MTA (Maden Tetkik ve Arama Genel Müdürlüğü)).....	69
Figure 8.4. Surface rupture, offset, cracks and damages on railway tracks and roads, as well as a damaged electric tower, near the surface rupture (Narlı, Kahramanmaraş). (Active fault data is taken from Emre et al. (2013)).....	70
Figure 8.5. A landslide and crack/damages on the road next to a water canal, causing significant lateral displacement of a concrete retaining wall (pushed towards the water canal), a tilt on an electric pole, in southern part of the city of Kahramanmaraş (active fault data from Emre et al. (2013)).....	70
Figure 8.6. Surface rupture observations causing a 3.6 m offset on Gaziantep-Kahramanmaraş road, cracks on the asphalt road at several locations, road embankment instability and more than 250 m-long longitudinal cracks at the top of the road embankment as well as on the asphalt road, near Kıpıçam, Kahramanmaraş (Satellite images are provided by Turkish General Directorate of Maps via atlas.harita.gov.tr website).....	71
Figure 8.7. Referring to Figure 6 for the location: surface rupture observations and 3.6 m offset on Gaziantep-Kahramanmaraş road (active fault data from Emre et al. (2013)).....	71
Figure 8.8. Landslides and surface cracks on the roads, near Kartal and Yarbaşı, Kahramanmaraş (Active fault data from Emre et al. (2013)).	72



Figure 8.9. Landslides, rockfalls and surface cracks on the roads, near Fevzipaşa, Gaziantep causing disruption in the service (Active fault data from Emre et al. (2013)).....	72
Figure 9.1 World heritage sites in and around Türkiye.....	76
Figure 9.2 Cities affected by the Kahramanmaraş earthquakes including Malatya and Elazığ....	76
Figure 9.3 Geographic location of the historic structures evaluated in Malatya and Elazığ.	78
Figure 9.4 Yeni Cami (new mosque) before and after pictures and short anchorage.	79
Figure 9.5 Gaziantep Castle before and after the earthquakes.....	80
Figure 9.6 The Antakya Rum Orthodox and Protestant Churches before and after earthquakes .	83
Figure 9.7 The Antakya Rum Orthodox Church after the earthquake	84
Figure 9.8 The Antakya Rum Protestant Church after the earthquake	84
Figure 10.1. Map Trends of activities and casualties between February 6 to 14, 2023	89

List of Tables

Table 1.1. Characteristics of $M_w=7.7$ Kahramanmaraş-Pazarcık Earthquake	14
Table 1.2. Characteristics of $M_w=7.6$ Elbistan Earthquake.....	14
Table 5.1. Identified Building Damage Distribution (Ministry of Environment, Urbanization and Climate Change)	45



Chapter 1.

Introduction

By:

Kemal Önder Çetin^(a), Ahmet Yakut^(a), Makbule İlgaç^(b), A. Arda Özacar^(a), Gizem Can^(c),
Elife Çakır^(a)

- (a) Middle East Technical University, Civil Engineering Department, Ankara, Türkiye
- (b) University of California, Civil and Environmental Engineering, Berkeley, USA
- (c) Royal Haskoning DHV Resilience& Maritime-BL Maritime & Water, Netherlands



1. 1. Introduction

On February 6, 2023, at 04:17 (01:17 GMT), a moment magnitude (M_w) 7.7 (AFAD, Disaster, and Emergency Management Presidency www.afad.gov.tr), earthquake occurred on the East Anatolian Fault. The epicenter of the Pazarcık-Kahramanmaraş-Türkiye Earthquake is located at N37.288°, E37.043° and approximately 40 km north-west of Gaziantep, and 33 km south-east of Kahramanmaraş, with a focal depth of 8.6 km (AFAD).

Following the first event, approximately 9 hours later, at 13:24 (10:24 GMT), an M_w 7.6 earthquake at Elbistan-Kahramanmaraş-Türkiye shook the region again. The epicenter of the second event is located at N38.089°, E37.239°, approximately 98 km north-west of Adıyaman, and 62 km north-east of Kahramanmaraş, with a focal depth of 7.0 km (AFAD). Both events took place on the East Anatolian Fault Zone (EAFZ), one of Türkiye's two major active fault systems. Figure 1.1 presents the locations of the epicenters.

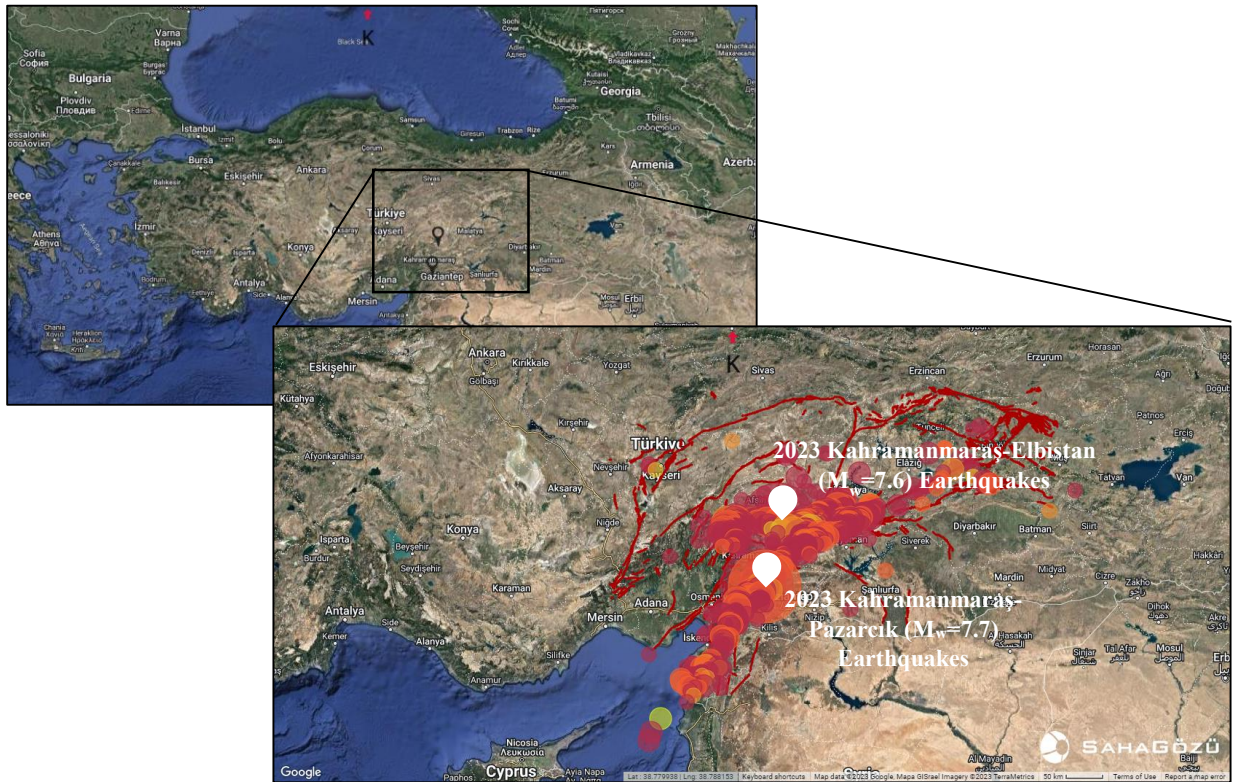






Figure 1.1. Map of Türkiye (Google Maps). The epicenter of the February 6, 2023, Kahramanmaraş-Pazarcık ($M_w=7.7$) and Kahramanmaraş-Elbistan ($M_w=7.6$) Earthquakes are shown with white pins.



The magnitude, depth, and source characteristics of these events are summarized in Tables 1.1 and 1.2, as reported by different national and international agencies. Consistent with the characteristics of the East Anatolian fault (EAF), the fault mechanism of the earthquakes is left-lateral strike-slip.

T

Institution	Focal Mechanism	Depth (km)	M_w
AFAD ¹	 b	8.6	7.7
KOERI ²	 l	10	7.7
USGS ³	 e	17.9	7.8
EMSC ⁴	 l	10	7.7




¹Turkish Prime Ministry-Disaster and Emergency Management Presidency

²Kandilli Observatory and Earthquake Research Institute

³United States Geological Survey

⁴European Mediterranean Seismological Centre

Table 1.2. Characteristics of $M_w=7.6$ Elbistan Earthquake

Institution	Focal Mechanism	Depth (km)	M_w
AFAD ¹	 b	7	7.6
KOERI ²	 l	10	7.6
USGS ³	 e	10	7.5
EMSC ⁴	NAV	10	7.5

¹Turkish Prime Ministry-Disaster and Emergency Management Presidency

²Kandilli Observatory and Earthquake Research Institute

³United States Geological Survey

⁴European Mediterranean Seismological Centre

Both events mostly affected the cities of Kahramanmaraş, Adıyaman, Hatay, Osmaniye, Gaziantep, Kilis, Şanlıurfa, Diyarbakır, Malatya, Adana, and Elazığ with residents of over 15 million. The events caused significant shaking and damage. As of 18.02.2023, the total number of casualties exceeded 40,000, and 110,000 were injured. More than 100,000 buildings collapsed or were heavily damaged.

A total number of 7451 aftershocks were recorded in the region as of 18.02.2023 within 200 km epicenter distance. 433 number of these aftershocks have magnitudes exceeding M_w 5.0 and 6.0, respectively. A total of 280 strong-motion stations, operated by AFAD, within 436 km from the zone of energy release, successfully recorded the February 6, 2023, Pazarcık-Kahramanmaraş



($M_w=7.7$) earthquake. The maximum peak ground acceleration (PGA) was reported as 1.23 g at Station 3126: Antakya. A total of 244 strong-motion stations, operated by AFAD and located within 445 km from the zone of energy release, recorded the second earthquake shaking. Similarly, the maximum PGA was reported as 0.65 g at station 4612: Kahramanmaraş Göksun. These aftershocks are also shown in Figure 1.1 along with the active fault lines and zones. A more detailed discussion regarding strong ground motion records is available in Chapter 3.

In response to the event, as part of the reconnaissance studies, the members of Middle East Technical University, Earthquake Engineering Research Center were mobilized to the region. These ongoing reconnaissance studies have covered an area of approximately 450 km by 100 km, including the mostly affected cities in Türkiye. The objective of this preliminary reconnaissance report is to share the effects of the event on the natural and built environment.

The first team accessed the area on February 7, the next day after the events, to collect and document perishable data in the form of structural damage, fault rupture, ground deformations, liquefaction manifestations, possible failure or non-failure performances of soil and rock slopes, buildings, retaining structures, ports, roads, bridges, airports, lifelines, hydraulic structures, and social impact. More specifically, the subsequent investigative efforts have mostly focused on documenting the followings:

- Background information related to the geology and seismo-tectonics of the region and geological field observations,
- Seismological background and processing of strong ground motions records,
- Detailed field reconnaissance information,
- Performance of residential structures,
- Performance of transportation systems including airports, railways, highways,
- Performance of bridges and tunnels,
- Foundation performance of buildings,
- Information on soil and rock slopes, seismic soil liquefaction manifestations, rockfalls, earth dams, harbors, lifelines, ports, deep excavations, retaining structures, industrial structures,
- Tsunami effects,
- Emergency response and community impact,



The preliminary reconnaissance findings regarding all these will be presented next. The opinions and conclusions presented in the report are the responsibility of the individual chapter authors and do not necessarily reflect the views of the entire report or the organization publishing it. A more detailed presentation of these findings will be available as part of the final reconnaissance report.

As the authors, we are deeply sorry for the loss of lives and injured citizens. We would like to convey our deepest condolences to the relatives of those who lost their lives during these events.



Chapter 2.

Regional Tectonics and Seismic Source

By:

A. Arda Özacar^(a), Bora Uzel^(b), Erdin Bozkurt^(a), Taylan Sançar^(c), Eyüp Sopaçlı^(a), Nuretdin Kaymakçı^(a), Bora Rojay^(a), Zeynep Gülerce^(d,*), Cem Kıncal^(b), Laura Gregory^(e).

- (a) Middle East Technical University, Geological Engineering Department, Ankara, Türkiye
- (b) Dokuz Eylül University, Geological Engineering Department, İzmir, Türkiye
- (c) Munzur University, Geography Department, Türkiye
- (d) Middle East Technical University, Civil Engineering Department, Ankara, Türkiye, currently in International Atomic Energy Agency (IAEA, Vienna)
- (e) University of Leeds, School of Earth and Environment, United Kingdom

*This is not an IAEA report and views expressed in any signed article do not represent those of the International Atomic Energy Agency and the IAEA accepts no responsibility for them.



2. 1. Regional Tectonics

East Anatolian Fault Zone (EAFZ) is about 450 km long, NE-trending left-lateral strike-slip fault system that lies between Karlıova and Hatay (Figure 2.1). The EAFZ is a major plate boundary, where the Arabian plate is moving towards the northeast with respect to the Anatolian plate at approximately 10-11 mm/yr (Çetin et al., 2003; Reilinger et al., 2006) with a total offset of 15-30 km (Şaroğlu et al., 1992; Westaway, 1994; 2003; Rojay et al. 2001; Moreno et al., 2011). It has been mostly neglected because it was seismically quiet for the last several decades. Some studies highlighted that this silence may be a manifestation of future events (e.g. Duman and Emre, 2013; Yönlü et al., 2013; Mahmoud et al., 2013; Karabacak and Altunel., 2013; Bayrak et al., 2015; Gülerce et al., 2017; Yönlü et al., 2017), its real seismic hazard potential has been seriously discussed by a vast of studies after the $M_w=6.8$ Elazığ earthquake in 2020 (e.g. Pousse-Beltran et al., 2020; Ragon et al., 2020; Tatar et al., 2020; Akgün and İnceöz, 2021; Doğru et al., 2021; Güvercin et al., 2022; Kelam et al., 2022; Akbayram et al., 2022).

2. 2. Major Earthquake History

The historical earthquakes along the EAFZ are partly synchronous, such that some of the segments slipped with similar magnitude earthquakes around the 19th century (Duman and Emre, 2013). The $M_w=7.8\pm 0.1$ Pazarcık and $M_w=7.7\pm 0.1$ Elbistan earthquakes have occurred on the EAFZ and caused devastating effects in the surrounding cities of Kahramanmaraş, Gaziantep, Malatya, Adıyaman, Hatay and Osmaniye. Based on historical data, fault segments ruptured during this earthquake sequence were seismic gaps with tectonic stress accumulating for at least 500 years (Ambraseys, 1989; Duman and Emre, 2013).

2. 3. Seismic Source

On February 6, 2023, 01:47 UTC, a large earthquake ($M_w: 7.8$) occurred near Pazarcık, Kahramanmaraş. The event hypocenter is located south of the EAFZ at 37.1123N, 37.1195E according to KOERI (Figure 2.1). Moment tensor solution revealed almost pure left-lateral strike-slip motion on a nearly vertical NE-SW trending fault. According to seismic data, this earthquake initiated on a smaller Narlı fault in the south jumped to the north and ruptured the Pazarcık-Erkenek fault segments towards NE and the Amanos segment towards SW with some time delay. This earthquake displays directivity effects over the edges of the rupture and discontinuous time



evolution along multiple fault segments and thus is a unique example of complex rupture displaying multi-event nature. The spatial distribution of aftershocks indicates that the earthquake rupture reached Antakya (Hatay) in the south and come to an end in the north at the Pütürge segment close to the Doğanyol, Elazığ earthquake in 2020 (Figure 2.1). The total rupture length is just over 300 km with major surface displacements on the order of 3 – 7 m. Ten minutes after the mainshock, a strong aftershock with $M_w6.8$ occurred just west of the mainshock's hypocenter, which may ruptured the Salçagöz fault.

Nine hours later (10:24 UTC), the Elbistan earthquake ($M_w7.7$) occurred along the Çardak-Sürgü fault segment, exhibiting a unique example of short-term earthquake triggering. The event hypocenter is located south of Elbistan near Ekinözü at 38.0717N, 37.2063E by KOERI (Figure 2.1). Like the previous event, the moment tensor solution suggested almost pure left-lateral strike-slip motion. Seismic data indicate that the earthquake initially ruptured the ~E-W trending Çardak fault which strike more southwards in the west and continued eastward towards Malatya on the NE-SW trending Doğanşehir fault zone. It is also worth noting that aftershocks on the western rupture tip are curving further down towards the south and imply possible activation of faults with different orientations (Figure 2.1). The total rupture length is around 160 km with major surface displacements on the order of 2 - 8 m.

2. 4. Surface Rupture and Geological Field Observations

Just after the earthquake sequence, surface ruptures were observed and mapped with open-access satellite images, aerial photographs provided by the General Directorate of Mapping (Türkiye), and field studies by geoscientists. Figure 2.2 displays left-lateral offsets observed on the roads at Güzelyurt and Pazarcık where displacement is about 2.4 m. Figure 2.3 shows displaced railway tracks near İslahiye along the Amanos segment and 6.7 m left-lateral fence offset documented along the Sürgü Segment.

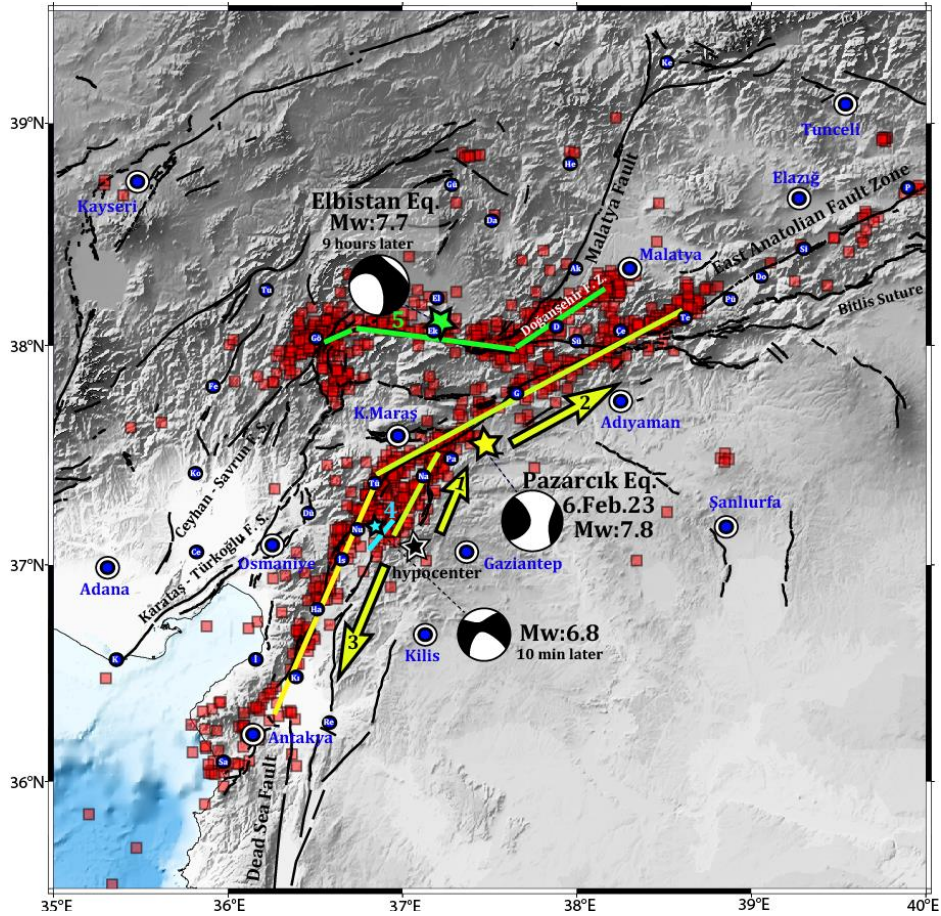


Figure 2.1. Examples Seismotectonic map showing rupture planes and aftershocks (taken from AFAD) along with global moment tensor solutions of recent major earthquakes. Ruptures are numbered in time and arrows indicate the inferred rupture direction of the initial Pazarcık earthquake ($M_w7.8$) which displays directivity and discontinuous rupture evolution.



Figure 2.2. Photos of 2.4 m road offset near Pazarcık and 6.7 m fence offset along the Sürgü-Çardak fault segment (taken by Erdin Bozkurt and Taylan Sançar respectively).



2. 5. Seismic Gaps and Static Stress Changes

This earthquake sequence displays a great example of short temporal seismic clustering, with two large earthquakes occurring closely in space and less than 10 hours apart in time. The estimated static stress changes using Coulomb failure along with historical earthquake records can point out the fault segments that become closer to failure. After the 2023 earthquake sequence, seismic gaps of EAFZ remain along the Savrun, Ceyhan, Kyrenia, Türkoğlu, Karataş, and Orontes fault segments in the south and on Gökdere push-up (Gülerce et al. 2017) located SW of Bingöl in the north. Preliminary static stress change calculations indicate noticeable stress increases, especially along Malatya, Savrun fault, and Orontes (Antakya) fault segments where tectonic stress has not been released by a large earthquake for a long time (Figure 2.3). Unfortunately, this earthquake sequence resulted in the greatest seismic tragedy to strike Türkiye in several decades, and future understanding using further data analysis will be critical for realistic seismic hazard assessment in Türkiye and worldwide.

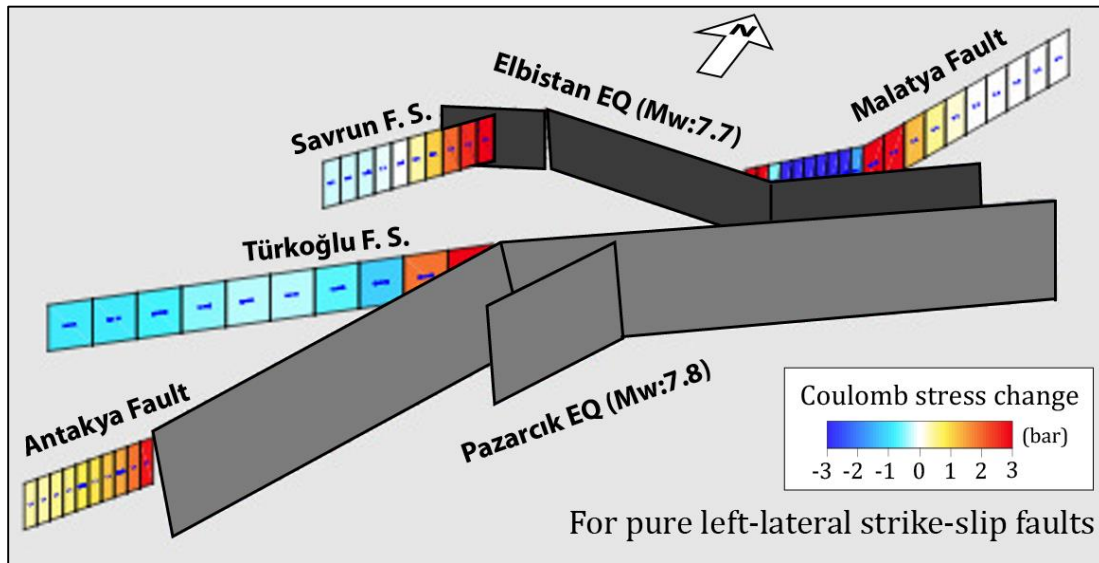


Figure 2.3. Coulomb static stress change on the neighboring fault segments after the recent earthquake sequence. Calculations were made for left-lateral strike-slip faults using finite fault solutions computed by USGS.



References

- Akbayram, K., Bayrak, E., Pamuk, E., Özer, Ç., Kıranşan, K., and Varolgüneş, S., 2022. Dynamic sub-surface characteristic and the active faults of the Genç District locating over the Bingöl Seismic Gap of the East Anatolian Fault Zone, Eastern Turkey. *Natural Hazards*, 114(1), 825-847.
- Akgün, E., and İnceöz, M., 2021. Tectonic evolution of the central part of the East Anatolian Fault Zone, Eastern Turkey. *Turkish J Earth Science*, 30, 928-947, doi:10.3906/yer-2104-15.
- Ambraseys, N.N., 1989. Temporary seismic quiescence: SE Turkey. *Geophysical Journal International*, 96(2), 311–331.
- Bayrak, E., Yılmaz, Ş., Softa, M., Türker, T., and Bayrak, Y., 2015. Earthquake hazard analysis for East Anatolian Fault Zone, Turkey. *Natural Hazards*, 76, 1063–1077, doi:10.1007/s11069-014-1541-53.
- Çetin, H., Güneyli, H. & Mayer, L. (2003) Paleoseismology of the Palu-Lake Hazar segment of the East Anatolian Fault Zone, Turkey. *Tectonophysics*, 374, 163-197.
- Doğru, A., Bulut, F., Yaltrak, C., and Aktuğ, B., 2021. Slip distribution of the 2020 Elazığ Earthquake (M_w 6.75) and its influence on earthquake hazard in the Eastern Anatolia. *Geophysical Journal International*, 224(1), 389-400.
- Duman, T.Y., Emre, Ö., 2013. The East Anatolian Fault: Geometry, segmentation and jog characteristics. *Geol. Soc. Spec. Publ.*, 372, 495–529. doi:10.1144/SP372.14.
- Gülerce, Z., Shah, S.T., Menekşe, A., Özacar, A.A., Kaymakci, N., and Çetin, K.Ö., 2017. Probabilistic seismic-hazard assessment for east anatolian fault zone using planar fault source models. *Bull. Seismol. Soc. Am.*, 107, 2353–2366, doi:10.1785/0120170009.
- Güvercin, S. E., Karabulut, H., Konca, A. Ö., Doğan, U., and Ergintav, S., 2022. Active seismotectonics of the East Anatolian Fault. *Geophysical Journal International*, 230(1), 50-69.
- Karabacak, V., and Altunel, E., 2013. Evolution of the northern Dead Sea Fault Zone in southern Turkey. *J. Geodynamics*, 65, 282–291. <http://dx.doi.org/10.1016/j.jog.2012.04.012>.
- Kelam, A.A., Karimzadeh, S., Yousefıbavil, K., Akgün, H., Askan, A., Erberik, M.A., Koçkar, M.K., Pekcan, O., and Ciftci, H., 2022. An evaluation of seismic hazard and potential damage in Gaziantep, Turkey using site specific models for sources, velocity structure and building stock. *Soil Dynamics and Earthquake Engineering*, 154, 107129.
- Mahmoud, Y., Masson, F., Meghraoui, M., Çakır, Z., Alchalbi, A., Yavasoglu, H., Yönlü, O., et al., 2013. Kinematic study at the junction of the East Anatolian Fault and the dead sea fault from GPS measurements. *Journal of Geodynamics*, 67, 30–39, doi:10.1016/j.jog.2012.05.006.
- Moreno, D.G., Hubert-Ferrari, A., Moernaut, J., Fraser, J.G., Boes, X., Van Daele, M., Avsar, U., Çağatay, N. and De Batist, M. (2011). Structure and recent evolution of the Hazar Basin: a strike-slip basin on the East Anatolian Fault, Eastern Turkey. *Basin Research* 23, 191-207.



- Pousse-Beltran, L., Nissen, E., Bergman, E.A., Cambaz, M.D., Gaudreau, É., Karasözen, E., and Tan, F., 2020. The 2020 Mw 6.8 Elazığ (Turkey) Earthquake Reveals Rupture Behavior of the East Anatolian Fault. *Geophys. Res. Lett.* 47, e2020GL088136, doi:10.1029/2020GL088136.
- Ragon, T., Simons, M., Bletery, Q., Cavalié, O., and Fielding, E., 2021. A Stochastic View of the 2020 Elazığ Mw 6.8 Earthquake (Turkey). *Geophys. Res. Lett.*, 48, doi:10.1029/2020gl090704.
- Reilinger, R., McClusky, S., Vernant, P., Lawrence, S., Ergintav, S., Cakmak, R. et al. (2006) GPS constraints on continental deformation in the Africa-Arabia-Eurasia continental collisional zone and implications for the dynamics of plate interactions. *Journal of Geophysical Research: Solid Earth*, 111(B5), B05411.
- Rojay, B., Heimann, A., and Toprak, V., 2001. Neotectonic and volcanic characteristics of the Karasu fault zone (Anatolia, Turkey): the transition zone between the Dead Sea transform and the East Anatolian fault zone. *Geodinamica Acta*, 14, 197–212.
- Şaroğlu, F., Emre, Ö. & Kuşçu, İ. (1992) The East Anatolian Fault zone of Turkey. *Ann. Tecton.*, 6, 99-125 (Special Issue-Supplement).
- Tatar, O., Sözbilir, H., Koçbulut, F., Bozkurt, E., Aksoy, E., Eski, S., Özmen, B., Alan, H., and Metin, Y., 2020. Surface deformations of 24 January 2020 Sivrice (Elazığ)–Doğanyol (Malatya) earthquake ($M_w=6.8$) along the Pütürge segment of the East Anatolian Fault Zone and its comparison with Turkey’s 100-year-surface ruptures. *Mediterranean Geoscience Reviews*, 2, 385-410.
- Westaway, R. (1994). Present-day kinematics of the Middle East and eastern Mediterranean. *J. Geophys. Res.*, 99, 12071-12090.
- Westaway, R. (2003). Kinematics of the Middle East and Eastern Mediterranean Updated. *Turkish J. Earth Sci.*, 12, 5-56.
- Yönlü, Ö., Altunel, E., Karabacak, V., and Akyüz, S.H., 2013. Evolution of the Gölbaşı basin and its implications for the long-term offset on the East Anatolian Fault Zone, Turkey. *Journal of Geodynamics*, 65, 272-281.
- Yönlü, O., Altunel, E., and Karabacak, V., 2017. Geological and geomorphological evidence for the southwestern extension of the East Anatolian Fault Zone, Turkey. *Earth Planet. Sci. Lett.*, 469, 1–14, doi:10.1016/j.epsl.2017.03.034.



Chapter 3.

Preliminary Analysis of Strong Ground Motion Characteristics

For the expanded version of this chapter please visit

https://eerc.metu.edu.tr/en/system/files/documents/CH4_Strong_Ground_Motion_Report_2023-02-20.pdf

By:

Zeynep Gülerce^(a,*), Ayşegül Askan^(b), Özkan Kale^(c), Abdullah Sandıkkaya^(d), Nihat Sinan Işık^(e), Okan İlhan^(f), Gizem Can^(g), Makbule Ilgaç^(h), A. Arda Özacar^(b), Kemal Önder Çetin^(b)

Burak Akbaş^(b), Abdullah Altındal^(b), Eyüp Sopacı^(b), Mehmet Fırat Aydın^(b), Baran Güryuva^(d), Onur Kanun^(b), Kubilay Albayrak^(b), Gamze Muratoğlu^(b), Oguz Salih Okçu^(d), Abdullah İçen^(j)

- (a) Middle East Technical University, Civil Engineering Department, Ankara, Türkiye, currently in International Atomic Energy Agency (IAEA, Vienna)
- (b) Middle East Technical University, Civil Engineering Department, Ankara, Türkiye
- (c) TED University, Civil Engineering Department, Ankara, Türkiye
- (d) Hacettepe University, Civil Engineering Department, Ankara, Türkiye
- (e) Gazi University, Civil Engineering Department, Ankara, Türkiye
- (f) Yildirim Beyazıt University, Civil Engineering Department, Ankara, Türkiye
- (g) Royal Haskoning DHV Resilience& Maritime-BL Maritime & Water, Netherlands
- (h) University of California, Civil and Environmental Engineering, Berkeley, USA
- (i) Atilim University, Civil Engineering Department Ankara, Türkiye
- (j) Munzur Üniversitesi, Civil Engineering Department Tunceli, Türkiye

*This is not an IAEA report and views expressed in any signed article do not represent those of the International Atomic Energy Agency and the IAEA accepts no responsibility for them.



3. 1. Introduction

The mainshocks of February 6, 2023, $M_w=7.7$ Kahramanmaraş-Pazarcık and $M_w=7.6$ Elbistan earthquakes and their aftershock sequences were recorded in a large region by the strong motion stations operated by AFAD (Disaster and Emergency Presidency of Türkiye). The recordings and station metadata are disseminated through AFAD's website, soon after both earthquakes (1st event at <https://tadas.afad.gov.tr/event-detail/15499> and 2nd event at <https://tadas.afad.gov.tr/event-detail/15512>, last accessed on February 12, 2023). The reconnaissance team downloaded the raw strong motion data immediately after they were available. However, sharing the responsibility of providing accurate data sets to the scientific and earthquake engineering community, updates in data by AFAD's personnel are being carefully monitored and changes have been implemented in this report as much as possible. It is clear that these recordings are currently evaluated by AFAD and improvements in data quality are expected in near future.

The longer version of this mini-chapter with detailed analyses of the full dataset from two events can be found at [here](#). In this preliminary report, selected ground motions from the first event are presented.

The data from February 6, 2023 earthquakes were compiled, analyzed for data quality, and processed with the procedures given in Akkar et al. (2014). After the visual quality control and data processing, 245 recordings from the first earthquake and 244 recordings from the second earthquake have remained in the database. Figures 3.1(a) and (b) show the spatial distribution of these recordings for both events, respectively. Figure 3.1 also presents the location of the epicenters (yellow stars) and the surface projections of the estimated rupture planes for each earthquake (for details, please refer to Chapter 2).

3. 2. Information on Recorded Strong Ground Motions at Selected Stations

Peak ground motion amplitudes, significant duration, and Arias as well as Housner intensity values of these recordings within $R_{RUP}<100\text{km}$ are provided in [here](#). Figure 3.2 display the data from the first event at the selected stations which are shown with red triangles in Figure 3.1. The 5%-damped acceleration response spectra in these figures are compared against the design spectra defined in the current seismic code of Türkiye (TBEC, 2019) for 475 and 2475-year return periods. For the other stations please see [here](#).

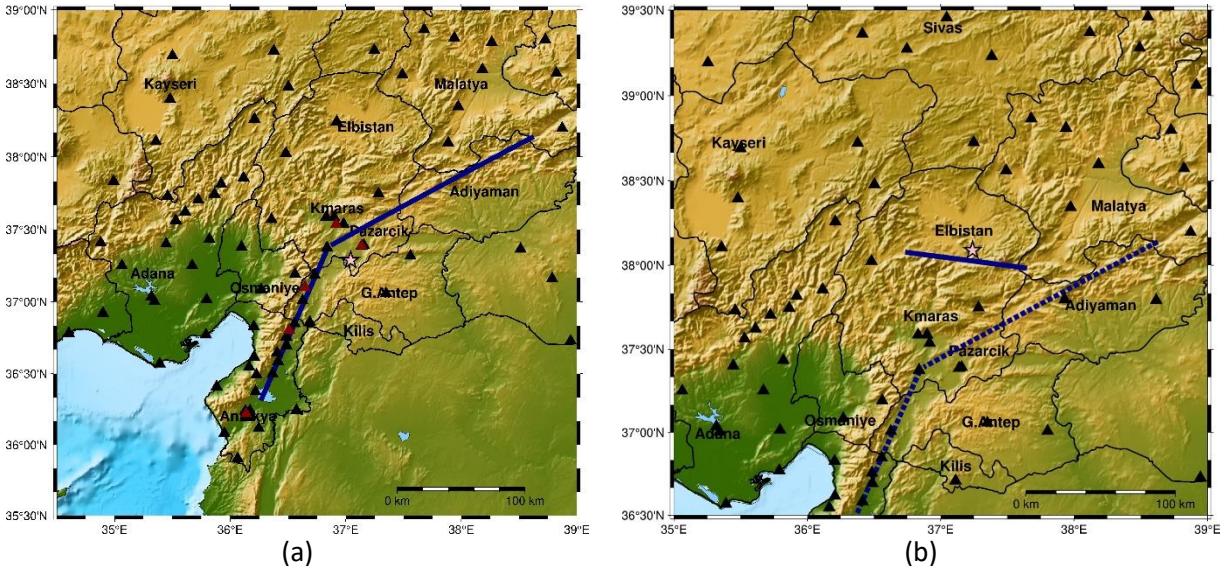


Figure 3.1. Distribution of the strong motion stations that are located within 200km of the rupture plane for (a) $M_w=7.7$ Kahramanmaraş-Pazarcık and (b) $M_w=7.6$ Elbistan earthquakes.

Station 2708 is located in İslahiye, Gaziantep, on a site with NEHRP site class C (site class ZC of TBEC, 2019) with a rupture distance of 4 km. We note that multiple wave packets are observed in the recorded accelerogram. Both the FAS and response spectra are computed based on the entire time series including all wave packets provided by AFAD. The maximum horizontal PGA is recorded in the EW direction as 1089 cm/s^2 . The vertical PGA value is recorded to be 977 cm/s^2 . The broadband nature of the response spectrum is attributed to multiple wave packets observed in this large event. Response spectra from both horizontal components show peaks in the short period range. Despite being located on stiff soil conditions; the response spectra of the EW component show clear amplifications also in the longer periods with a particular peak around 1.2 seconds. The geometric mean of two horizontal response spectra exceeds the design spectrum corresponding to a return period of 475 years at almost all periods. The same geometric mean exceeds the design spectrum for a return period of 2475 years for periods longer than 0.7 seconds. We note that there are severe damages and collapses around this region based on the first observations in the field.

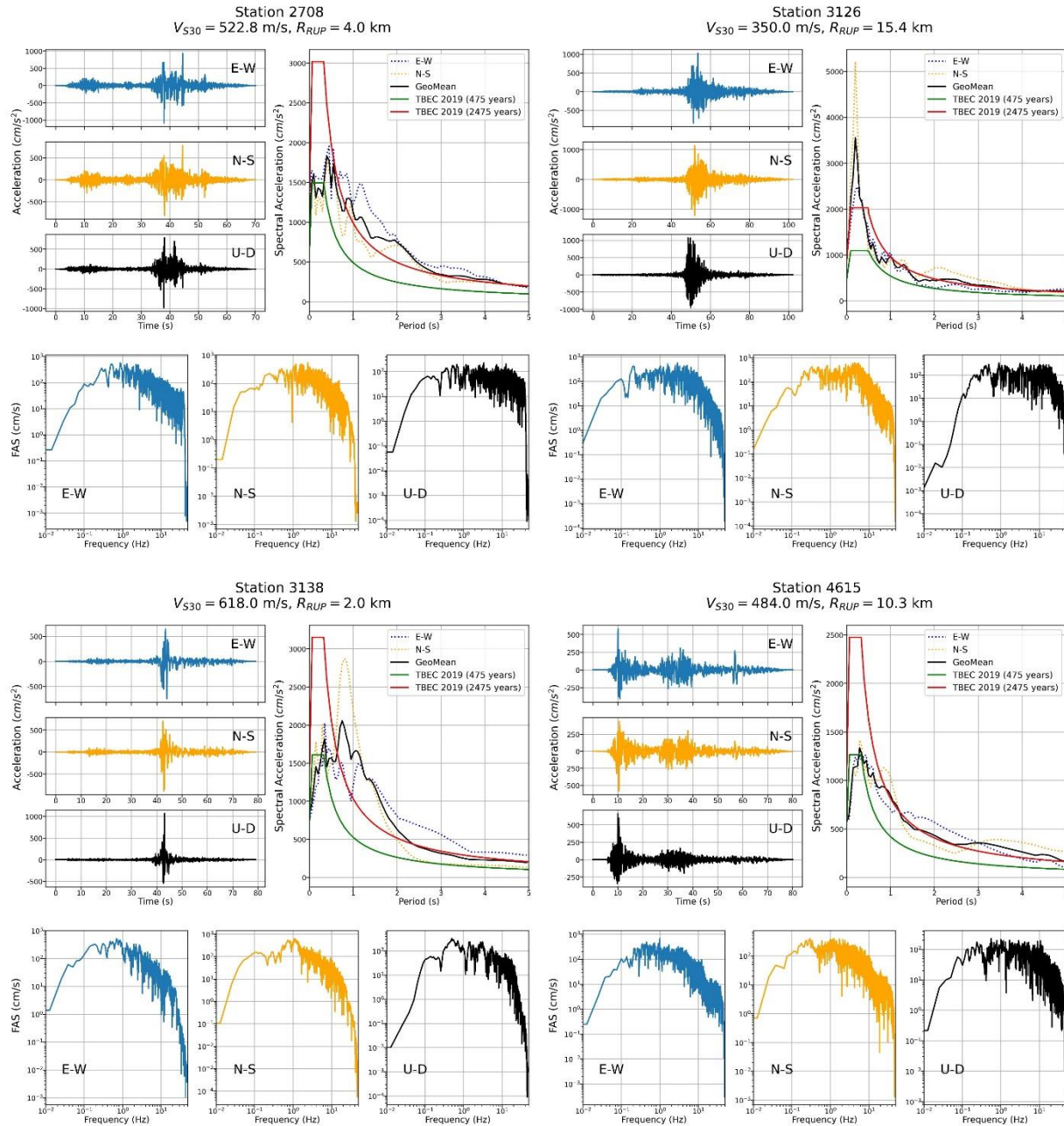


Figure 3.2. Recorded three-component ground accelerations, corresponding Fourier amplitude spectra (FAS), and response spectra (with 5% damping) in comparison with the most recent building code (TBEC, 2019) at selected stations due to Pazarcık ($M_w=7.7$) event

Station 3126 is located in Antakya, on a site with NEHRP site class D (site class ZD of TBEC, 2019) with a rupture distance of 15.4 km. The maximum horizontal PGA is recorded in the NS direction as 1210 cm/s^2 . The vertical PGA value is 1070 cm/s^2 . We observe that the accelerations



recorded in the vertical direction are similar to the horizontal ones in terms of frequency and amplitude contents. The response spectra of both EW and NS components indicate amplifications around 0.3 seconds and they both exceed the design spectrum for a return period of 475 years. The geometric mean is above the design spectrum for a return period of 2475 years for periods less than 0.4 seconds and below for longer periods.

Station 3138 is located in Hassa, Hatay on a site with NEHRP site class C (site class ZC of TBEC, 2019) with a rupture distance of 2 km. The acceleration records point out potential directivity effects. When velocities are investigated, this record indicates forward directivity effects characterized by short duration and high amplitude two-sided long-period velocity pulses. The geometric mean of horizontal response spectra indicates broadband period content and exceeds the design spectrum for a return period of 475 years for periods longer than 0.4 seconds.

Station 4615 is located in Pazarcık on a site with NEHRP site class C (site class ZC of TBEC, 2019) at a rupture distance of 10.3 km. This record also displays broadband response spectra possibly due to the multiple wave packets. The maximum PGA value is recorded in the vertical component as 664 cm/s^2 . The geometric mean spectrum is observed to exceed the 475-year design spectrum at periods larger than 0.5 s, and it is shown to be similar to the 2475-year design spectrum at periods larger than 1 s.

3. 3. Spatial Distribution of Peak Ground Parameters from February 6 Earthquakes

Figure 3.3 and 3.4 summarizes the spatial distribution of peak ground acceleration and velocity values from the Pazarcık and Elbistan earthquakes, respectively. When Figure 3.3 is investigated, it is observed that the highest PGA values are recorded in Antakya, while very high PGA values between $500\text{-}1000 \text{ cm/s}^2$ are observed generally in the North-South direction, covering the provinces of Kahramanmaraş, Gaziantep, Osmaniye, Kilis, and Hatay. The distribution of PGV values is more homogeneous compared to the PGA, with very high intensities at all stations close to the rupture. The second event, Elbistan earthquake ($M_w=7.6$), is not as densely-recorded as the Pazarcık ($M_w=7.7$) event. As the rupture is located to the north of the first event (Figure 3.4), the effects of this event are felt more noticeably in the northern provinces in addition to Kahramanmaraş, such as Adıyaman, Malatya, and Kayseri. The highest ground motion intensities are generally observed in Kahramanmaraş.

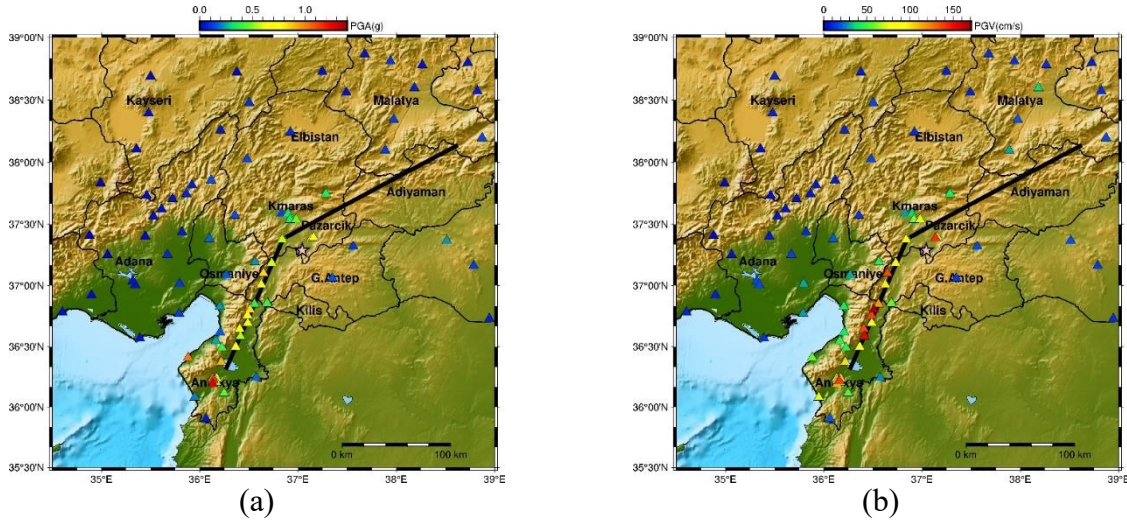


Figure 3.3. Spatial distribution of intensity measure of Pazarcık earthquake (a) PGA, (b) PGV

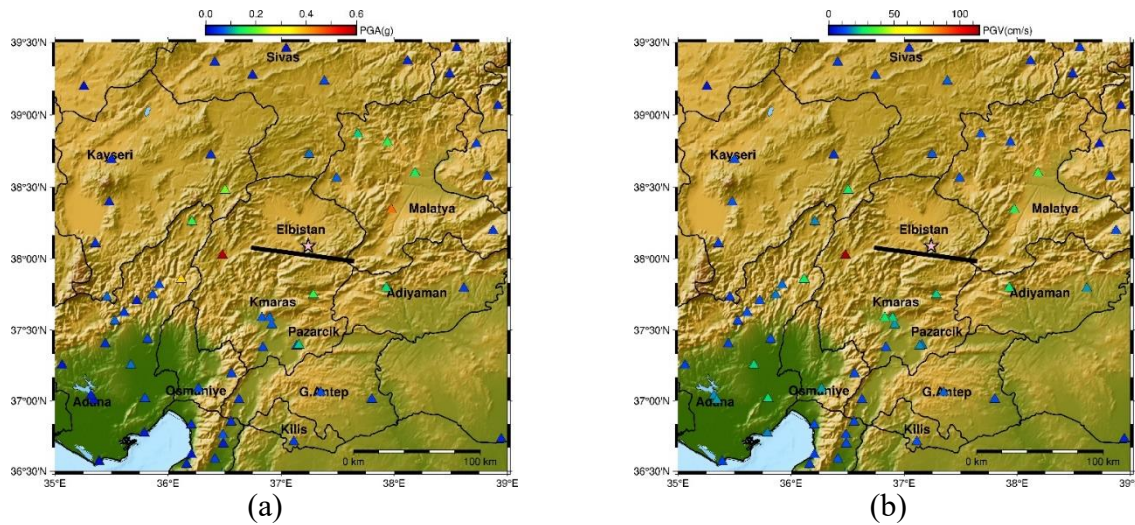


Figure 3.4. Spatial distribution of intensity measure of Elbistan earthquake (a) PGA, (b) PGV

Finally, for detailed analyses of recorded strong ground motion data at other stations, information on felt intensity values, comparisons against ground motion models, and initial analyses on site amplifications please see [here](#).

References

Akkar, S., Sandikkaya, M.A., Şenyurt, M., Azari Sisi, A., Ay, B.Ö., Treversa, P., Douglas, J., Cotton, F., Luzi, L., Hernandez, B., Godey, S. 2014. “Reference Database for Seismic Ground Motion in Europe (RESORCE)”. *Bulletin of Earthquake Engineering*, 12:311–339. <https://doi.org/10.1007/s10518-013-9506-8>

Turkish Building Earthquake Code (TBEC) 2019. Ministry of Interior, Disaster and Emergency Management Presidency (AFAD), Ankara, Türkiye.



Chapter 4.

Geotechnical Findings and the Performance of Geo-Structures

By:

Kemal Önder Çetin^(a), Candan Gökçeoğlu^(b), Robb Eric Shedwick Moss^(c), Makbule Ilgaç^(d), Gizem Can^(e), Elife Çakır^(a)

Bilal Umut Aydın^(a), Arda Şahin^(a), Mehmet Türkezer^(a), Berkan Söylemez^(a), Soner Ocak^(a), Hayri Güzel^(a),

(a) Middle East Technical University, Civil Engineering Department, Ankara, Türkiye

(b) Hacettepe University, Geological Engineering Department, Ankara, Türkiye

(c) California Polytechnic State University, Civil and Environmental Engineering, San Luis Obispo, USA

(d) University of California, Civil and Environmental Engineering, Berkeley, USA

(e) Royal Haskoning DHV Resilience& Maritime-BL Maritime & Water, Netherlands



4. 1. Geotechnical Observations

This chapter presents the preliminary findings of ongoing geotechnical reconnaissance studies after the earthquakes. Several geotechnical reconnaissance teams were mobilized to the field to collect and document perishable data. More specifically, these discussions will focus on the documentation and preliminary assessments of geotechnical aspects, which are listed as i) seismic soil liquefaction, ii) foundation performance, iii) deep excavations, iv) retaining structures, v) rockfall, vi) tunnel performance, vii) slope stability, and viii) ground deformations, and ix) faulting induced pipeline breakage.

4. 1. 1. Seismic Soil Liquefaction Manifestations

Seismic soil liquefaction-induced surface manifestations in the form of ejecta, lateral spreading, and subsidence were observed, as displayed in Figure 4.1 through Figure 4.3. Some of these manifestations were observed as in Figure 4.1 at free field sites. In addition to free field sites, liquefaction surface manifestations were also observed in the vicinity of building foundations. Figure 4.3 display the ejecta observed at the edges of residential building foundations.

The liquefaction phenomena were widely observed in Hatay-Paşaköy, Hatay-İskenderun, Adıyaman-Gölbaşı, Adıyaman-Türkoğlu regions. Lateral spreading and subsidence were accompanied to liquefaction triggering at these sites.



(a)



(b)



(c)

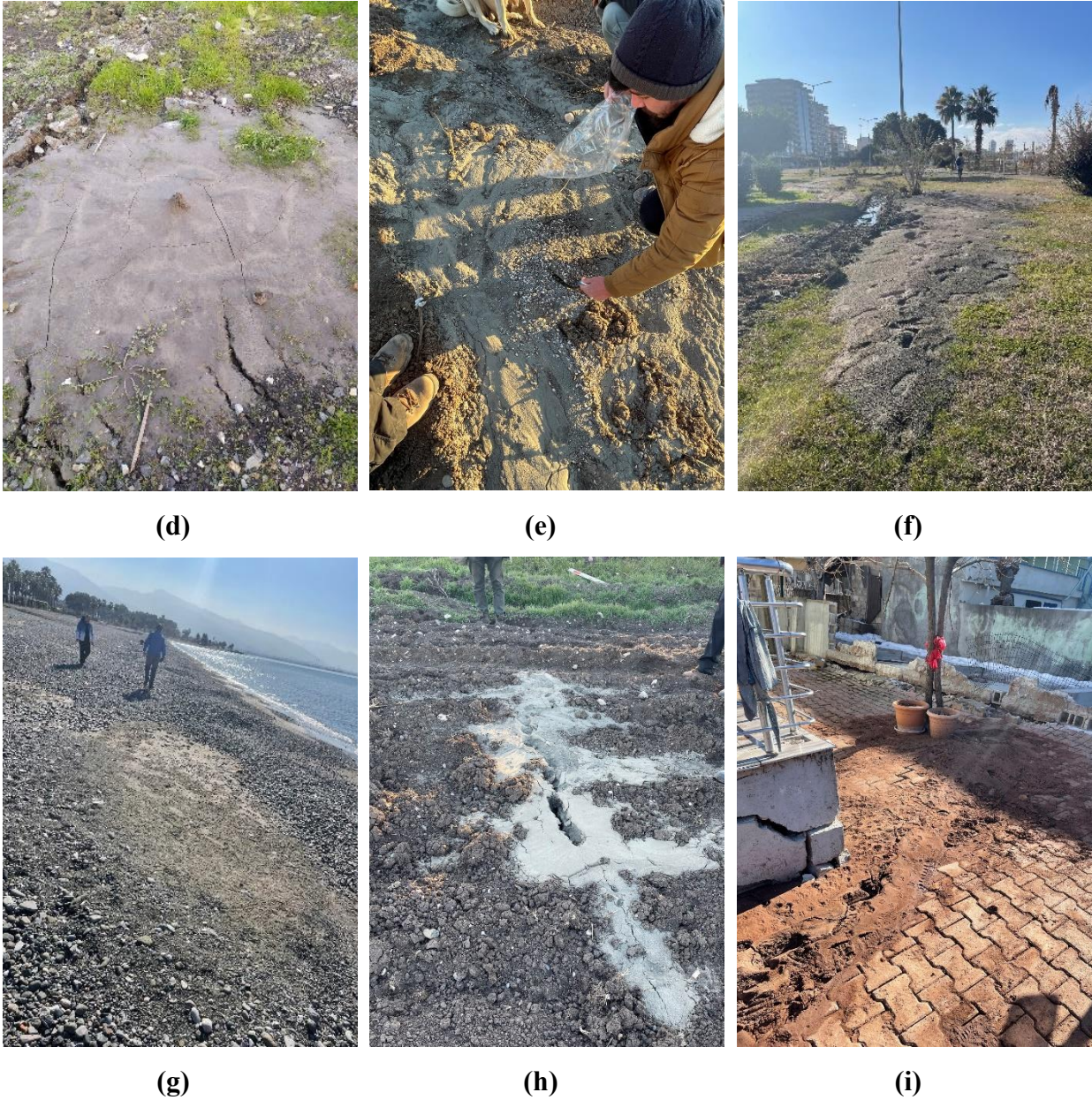


Figure 4.1. Seismic soil liquefaction-induced surface manifestation: sand boils in free field conditions: **a)** Hatay ($36.36446^\circ N, 36.28147^\circ E$), **b)** Kumlu / Hatay ($36.35628^\circ N, 36.39360^\circ E$), **c)** Fatih District / Gölbaşı / Adıyaman ($37.78080^\circ N, 37.62888^\circ E$), **d)** İskenderun / Hatay ($36.59323^\circ N, 36.18542^\circ E$), **e)** Emiroğlu / Kahramanmaraş ($37.33689^\circ N, 37.04538^\circ E$), **f)** Çay District / İskenderun / Hatay ($36.59133^\circ N, 36.17888^\circ E$) **g)** Dört Yol / Hatay ($36.81878^\circ N, 37.17770^\circ E$) **h)** Emiroğlu / Kahramanmaraş ($37.33722^\circ N, 37.04549^\circ E$) **i)** Gölbaşı / Adıyaman ($37.78655^\circ N, 37.63155^\circ E$)



(a)



(b)



(c)



(d)



(e)



(f)

Figure 4.2. Seismic soil liquefaction induced lateral spreadings in **a)** Çay District / İskenderun / Hatay ($36.59281^{\circ}N$, $36.185977^{\circ}E$), **b)** Özerli District / Dörtyol / Hatay ($36.81294^{\circ}N$, $36.18123^{\circ}E$), **c)** Fatih District / Gölbaşı / Adıyaman ($37.78023^{\circ}N$, $37.62858^{\circ}E$), **d)** İskenderun Port Area / Hatay ($36.59991^{\circ}N$, $36.19274^{\circ}E$), **e)** İskenderun Port Area / Hatay ($36.59991^{\circ}N$, $36.19274^{\circ}E$), **f)** İskenderun Port Area / Hatay ($36.59991^{\circ}N$, $36.19274^{\circ}E$).



(a)



(b)



(c)



(d)

Figure 4.3. Seismic soil liquefaction-induced induced foundation problems in **a)** Çay District / İskenderun / Hatay ($36.5911^{\circ}N$, $36.1790^{\circ}E$), **b)** Çay District / İskenderun / Hatay ($36.5911^{\circ}N$, $36.1790^{\circ}E$), **c)** Çay District / İskenderun / Hatay ($36.5911^{\circ}N$, $36.1790^{\circ}E$), **d)** Çay District / İskenderun / Hatay ($36.5911^{\circ}N$, $36.1790^{\circ}E$)



4. 1. 2. Residential Building Foundation Performance

Many residential building foundations in Hatay-İskenderun, and Adıyaman-Gölbaşı regions were subjected to excessive settlements and bearing capacity failures due to seismic soil liquefaction initiation. The extent of these foundation settlements varies in the range of a couple of centimeters to an excess of 80 cm. Moreover, differential settlements reach 30 cm, causing 5 to 10 degree tilting of buildings. An extreme case of liquefaction-induced bearing capacity failure and toppling of a residential building in Adıyaman-Gölbaşı is shown in Figure 4.4 (e). Raft foundation thickness of this building is measured as 80 cm.



Figure 4.4. Poor foundation performance in **a)** Çay District / İskenderun / Hatay ($36.5911^{\circ}N$, $36.1790^{\circ}E$), **b)** Hüriyet District / Gölbaşı / Adıyaman ($37.778^{\circ}N$ $37.628^{\circ}E$), **c)** Yavuz Selim District / Gölbaşı / Adıyaman ($37.788^{\circ}N$, $37.642^{\circ}E$), **d)** Yavuz Selim District / Gölbaşı / Adıyaman ($37.788^{\circ}N$, $37.642^{\circ}E$), **e)** Yavuz Selim District / Gölbaşı / Adıyaman ($37.78827^{\circ}N$ $37.64879^{\circ}E$)

4. 1. 3. Deep Excavations

The performance of deep excavation systems on the route was also investigated. Figure 4.5 (a) and (b) display Osmaniye-Bahçe underpass, which was supported by cantilever reinforced concrete pile elements. No significant deformations were observed in the deep excavation support system. Next to the site, there exists a tunnel portal structure. Figures 4.5 (c) and (d) show the portal structure supported by reinforced concrete piles and strut elements.



(a)



(b)



(c)



(d)

Figure 4.5. Examples of deep excavations in **a)** Bahçe / Osmaniye ($37.18845^\circ N$, $36.56326^\circ E$), **b)** Bahçe / Osmaniye ($37.18939^\circ N$, $36.56402^\circ E$), **c)** Bahçe / Osmaniye ($36.17313^\circ N$, $36.59912^\circ E$), **d)** Bahçe / Osmaniye ($36.17313^\circ N$, $36.59912^\circ E$)

4. 1. 4. Retaining Structures

A limited number of tilted and/or partially collapsed and collapsed walls were also observed. Some stone walls supporting highway cuts and fills were deformed or fully collapsed as shown in Figures 4.6 (a) and (b). However, mechanically stabilized earth fill walls widely used as approach fills for bridges perform extremely well under peak ground acceleration levels in excess of 1 g in Fevzipaşa as shown in Figures 4.6 (c) and (d).



(a)



(b)



(c)



(d)

Figure 4.6. Some examples of retaining structures in **a)** Gökçedere/ Gaziantep ($37.16439^\circ N$, $36.70672^\circ E$), **b)** Gökçedere/ Gaziantep ($37.16546^\circ N$, $36.69749^\circ E$), **c)** Bahçe/ Osmaniye ($37.18853^\circ N$, $36.56389^\circ E$), **d)** Bahçe/ Osmaniye ($37.18844^\circ N$, $36.56476^\circ E$)

4. 1. 5. Rockfalls

Several rockfalls were observed by the benches of highways and some examples are shown in Figures 4.7 (a) through (d).

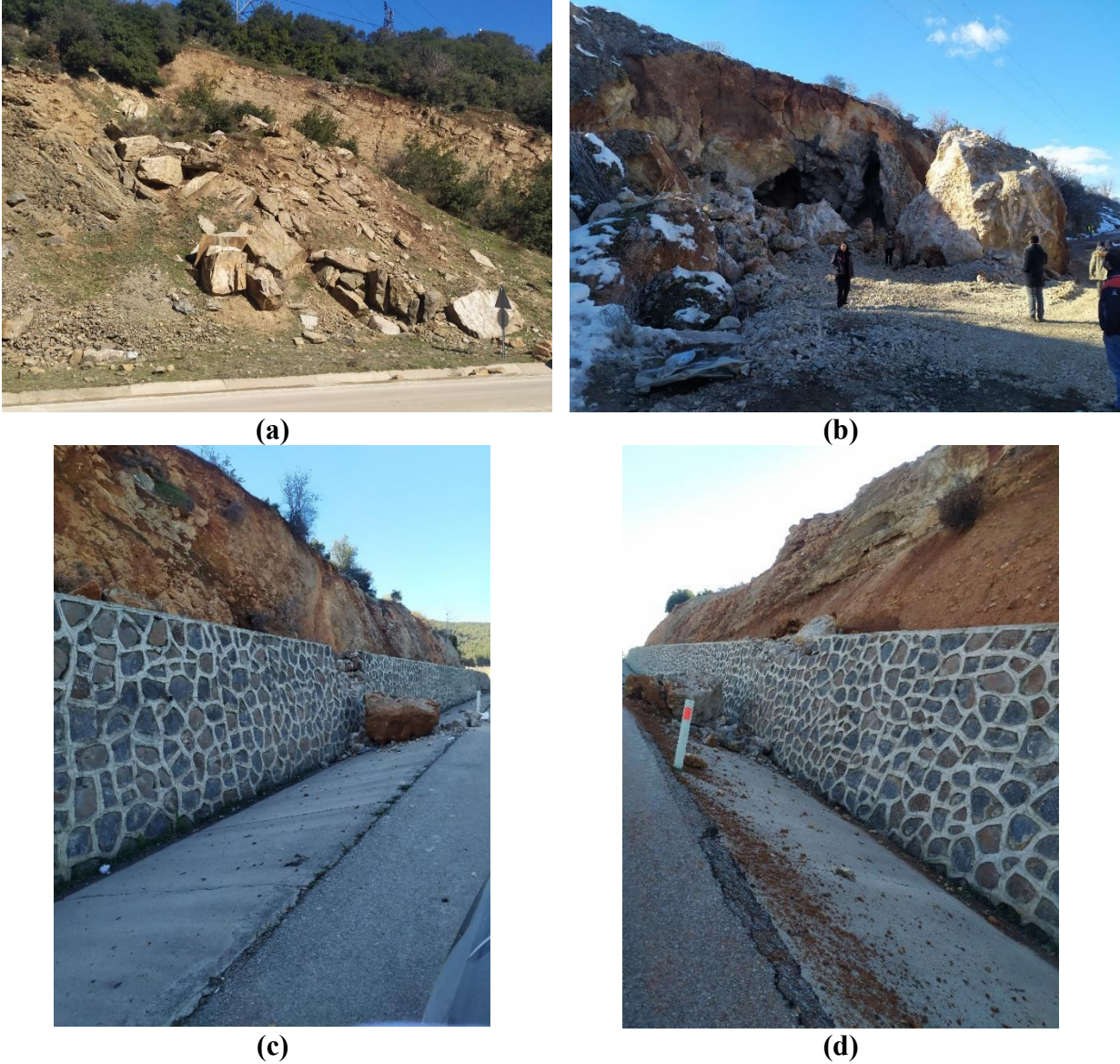


Figure 4.7. Some examples of rockfalls in **a)** Bahçe / Osmaniye ($37.17441^{\circ}N, 36.65659^{\circ}E$), **b)** Yolbağı District / Adıyaman ($37.81795^{\circ}N, 37.63311^{\circ}E$), **c)** Fevzi Paşa District / İslahiye /Gaziantep ($37.09899^{\circ} N, 36.65200^{\circ} E$), **d)** Fevzi Paşa District / İslahiye /Gaziantep ($37.09713^{\circ} N, 36.65170^{\circ} E$)

4. 1. 6. Tunnels

Tunnel structures in general performed well during and after the event. Except for minor damage observed in Erkenek tunnel lining, no major deformations were mapped. Some pictures from ongoing Bahçe-Nurdağ railway tunnel construction site are shown in Figure 4.8. The structural and geotechnical performance of them is reported to be superior. More about tunnels will be discussed in Chapter 6.



Figure 4.8. Bahçe-Nurdağı railway tunnels under construction in Nurdağı/ Gaziantep (37.16989°N, 36.70806°E)

4. 1. 7. Landslides

Several landslides with dimensions varying from a scale of a couple of meters to hundreds of meters were documented as part of reconnaissance studies. Some of these are shown in Figures 4.9 (a) through (c).

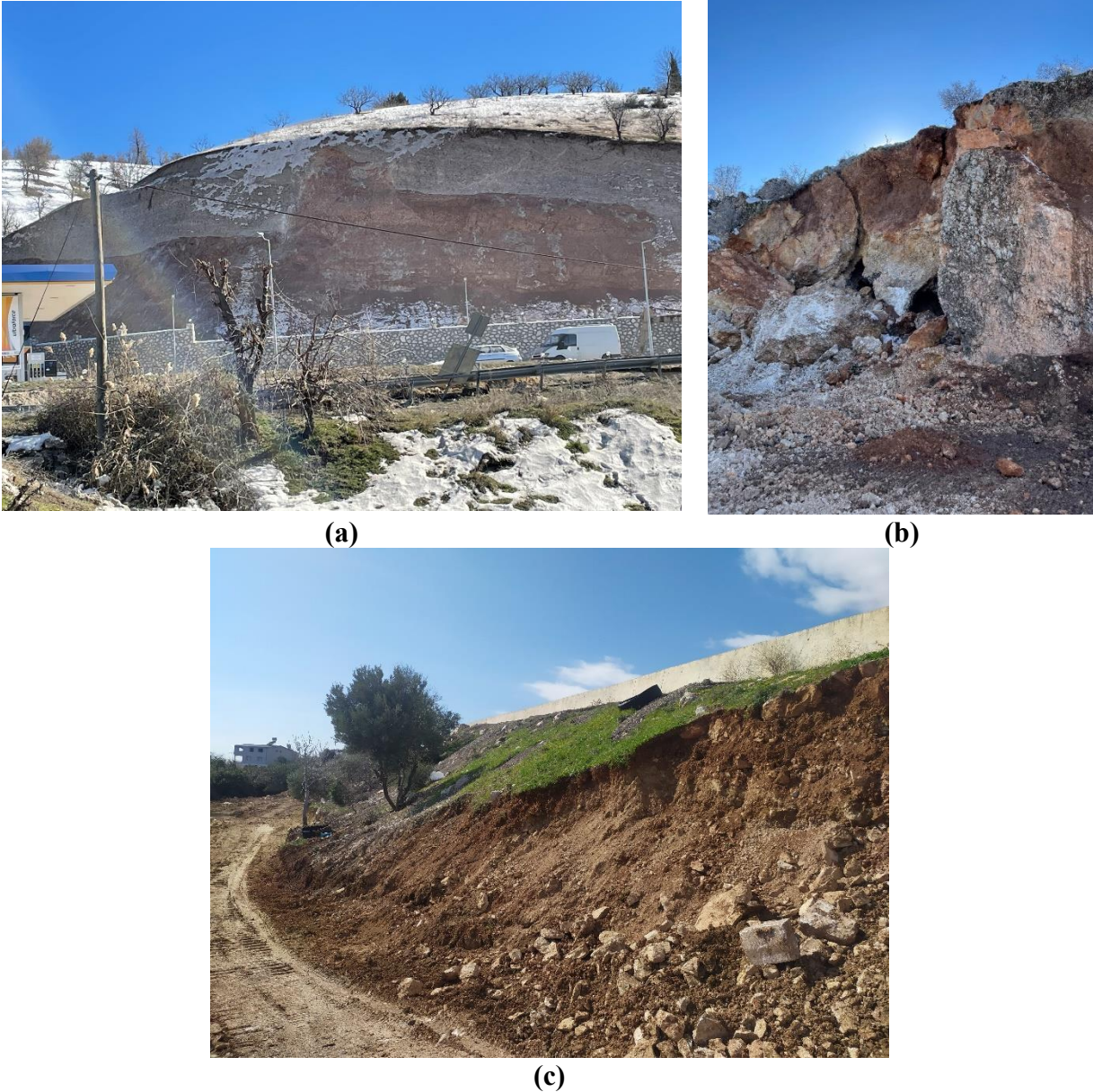


Figure 4.9. Some examples of slope stability problems in **a)** Gölbaşı/ Adıyaman ($37.79783^{\circ}N$, $37.66232^{\circ}E$), **b)** Yolbağı District / Adıyaman ($37.81806^{\circ}N$, $37.63297^{\circ}E$), **c)** Belen / Hatay ($36.48363^{\circ}N$, $36.27158^{\circ}E$)

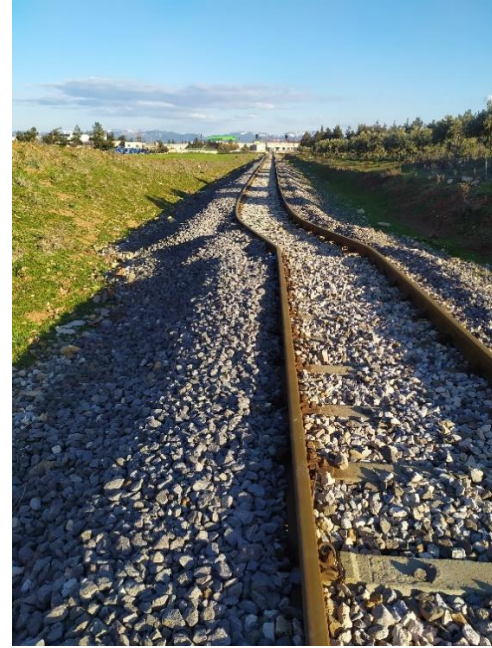


4. 1. 8. Ground Deformations

Along the route, several ground deformations either due to primary, secondary, or tertiary faulting or due to seismic soil liquefaction were mapped. Figures 4.10 (a) through (d) display these ground deformations.



(a)



(b)



(c)



(d)

Figure 4.10. Observation of surface rupture trace in **a)** Balkar / Adıyaman ($37.73610^{\circ}N$, $37.56842^{\circ}E$), **b)** Erenler District / İslahiye / Gaziantep ($37.03931^{\circ}N$, $36.62868^{\circ}E$), **c)** Yavuz Selim District / Adıyaman ($37.79645^{\circ}N$, $37.66021^{\circ}E$), **d)** Balkar / Adıyaman ($37.73492^{\circ}N$, 37.56617°)



4. 1. 9. Faulting induced Pipeline breakage

Pipelines were observed to be damaged after the earthquakes and some examples of the damaged pipeline and cables are shown in Figures 4.11 (a) and (b).



(a)



(b)

Figure 4.11. Pipeline damages in a) Erenler District / İslahiye / Gaziantep ($36.04621^{\circ}N$, $36.62936^{\circ}E$), b) Çay District / İskenderun / Hatay ($36.59038^{\circ}N$, $36.17893^{\circ}E$)

Acknowledgments: We would like to acknowledge the funding provided for the fieldwork by The Scientific and Technological Research Institution of Türkiye (TÜBİTAK) “1002-C Natural Disasters-Focused Fieldwork Emergency Support Program (Doğal Afetler Odaklı Saha Çalışması Acil Destek Programı)”.



Chapter 5.

Performance of Residential Structures

By:

Barış Binici^(a), Ahmet Yakut^(a), Erdem Canbay^(a), İsmail Ozan Demirel^(a), Mevlüt Kahraman^(b), Altuğ Erberik^(a), İsmail Özgür Yaman^(a), Eray Baran^(a), Afşin Canbolat^(c), Koray Kadaş^(c), Orkun Öztaşkın^(c), Selin Aktaş^(a)

(a) Middle East Technical University, Civil Engineering Department, Ankara, Türkiye

(b) Bilkent University, Construction works, Ankara, Türkiye

(c) Middle East Technical University, Office of Revolving Funds (DSIM), Ankara, Türkiye



5. 1. Performance of Buildings

Pazarcık and Elbistan-Kahramanmaraş earthquakes were one of the most destructive earthquakes, if not the most, experienced in Türkiye in the last century. Unlike previous earthquakes for which the damage has usually concentrated in a certain city, the building damage spread to eleven cities. The building damage inventory collected as of February 16, 2023, is given in Table 5.1. Based on this inventory, Hatay, Kahramanmaraş, Gaziantep, Adıyaman and Malatya experienced extensive damage due to the proximity of these cities to the faults, whereas the number of buildings collapsed in Kilis, Adana, Diyarbakır, Osmaniye, Şanlıurfa and Elazığ is smaller.

The intensity of the ground motion, the structural system, design, and construction quality were decisive in the building performance. The acceleration response spectra for the recorded motions in Göksun, Kahramanmaraş, Narlı, Hatay, Fevzipaşa, Malatya are presented in Chapter 3. It can be observed that design response spectra for residential buildings (i.e. maximum design earthquake with a return period of 475 years) are exceeded for a wide period range, whereas the maximum credible earthquake level (return period of 2475 years) response spectra is generally exceeded for long periods especially in soft soils, in certain regions. This implies that in Gaziantep (İslahiye and Nurdağı districts), Hatay, Kahramanmaraş, and Adıyaman the buildings were subjected to seismic actions larger than Turkish Earthquake Code design levels.

The building damage inventory in the region can be divided into two, based on their construction periods. A significant change is believed to occur in Türkiye between 1998 and 2001 due to the following four factors:

- A modern earthquake code was put into effect on September 2, 1998,
- Two destructive earthquakes occurred on August 17, and November 12, 1999, in Kocaeli and Düzce awakening awareness for seismic resistance,
- A modern reinforced concrete design guideline (TS-500) come to force on October 12, 2000, making ready mix concrete and ductile low carbon content steel as reinforcement,
- Building Inspection Law enacted on July 13, 2001, for 19 pilot cities including Gaziantep and Hatay. This law was extended to the whole country in 2010.

We divided our reconnaissance into two groups: reinforced concrete (RC) buildings constructed before and after 2002, based on the information collected at the building sites.



Table 5.1. Identified Building Damage Distribution (Ministry of Environment, Urbanization and Climate Change)

Damage State	Hatay	K.maraş	Adiyaman	Malatya	Gaziantep	Kilis	Adana	Diyarbakır	Osmaniye	Şurfa	Elazığ
None	29188	25420	21365	7463	89092	2849	1688	18039	22041	19585	9503
Light	17212	20556	38823	8960	29471	2208	5314	6725	8034	13507	15532
Moderate	2827	1058	2613	945	4361	137	304	713	266	550	138
Heavy/Collapse Urgent Demolish	15248	12980	6990	8365	12964	812	59	643	2531	466	664

5. 1. 1. Performance of RC Buildings Before 2000

Typical deficiencies of the frame buildings constructed before 2000 were the use of smooth reinforcing bars, insufficient steel reinforcement detailing and possibly low concrete strength resulting in heavy damage and collapse (Figure 5.1). The presence of soft story in the ground level or above the plinth was one of the key reasons of collapse in many buildings. The use of the ground floors as commercial stores with little or no infill walls were responsible for plastic hinging in columns occurred resulting in pancake type collapse as observed in previous earthquakes (Kocaeli 1999, Van 2011). This is displayed in Figure 5.2. Several buildings have experienced beam-column joint failures. Another interesting type of failure was the overturning of the building from its base due the inability of transferring lateral forces to the foundation (Figure 5.3).



Figure 5.1. Building Collapse in Antakya and Kahramanmaraş



Figure 5.2. Building Collapse in Malatya



Figure 5.3. Overturning due to soil liquefaction and insufficient joint reinforcement detailing

5. 1. 2. Performance of RC Buildings After 2000

These buildings presumed to be designed and constructed according to the codes performed better than the older buildings. However, more than 1000 buildings constructed after 2000 were heavily damaged or collapsed violating the code given performance objective. This appears to be an important observation demanding further investigations on the design and construction quality of those buildings. Some examples of these heavily damaged buildings are shown in Figure 5.4. The possible reasons for these damages can be attributed to i) the use of flexible joist slabs as diaphragms, ii) insufficient engineering design to distribute lateral forces to vertical load bearing elements perhaps due to the blind use of building design softwares, iii) possible detailing errors on building construction site, iv) underestimation of seismic demands, iv) insufficient investigations geotechnical site investigations prior to building construction and poor foundation design especially in Hatay and Gölbaşı regions. Such heavy damage observed in new buildings bring concerns about the target seismic performance of residential buildings nearly in compliant with the current seismic code. The significant disruption of city life, heavy monetary loss, and long recovery times may require reassessing the performance targets of buildings.



Tunnel form buildings in the region performed in an outstanding manner (Figure 5.5) with some damage in the coupling beams and infill walls due to the following key reasons: i) the use of more shear wall area more than usually 2.5% of the floor area, ii) siting at stiff soil or rock sites, iii) mid-rise construction ranging from (4 to 8 stories). This performance provided further confidence in the use of significant shear wall area for the buildings constructed in high seismic zones.



Figure 5.4. Heavily damaged new buildings in Adıyaman and İslahiye



Figure 5.5. Performance of a tunnel form building

5. 1. 3. Performance of Precast Buildings

Industrial Regions in Kahramanmaraş and Gaziantep have many precast concrete buildings with one or two stories. Typical main direction of the buildings has a span of about 20 m, and the other direction has a span of 7.5 m. The story heights vary between 7 to 10 m. The building frame columns are fixed at the base with a socket connection, whereas the prestressed (for long spans) roof girders are pinned to the column corbels usually with two grouted anchors embedded into the corbels. Typical buildings are shown in Figure 5.6. Two buildings that were under construction collapsed due to overturning of the girders. The failure is assumed to be initiated at the pin connections under the lateral force demands. Interestingly no indication of column base hinging was observed. In Gaziantep, most of the prefabricated buildings showed satisfactory performance.



In a few lightly damaged buildings, the typical damage was observed in column corbels due to the girder rotations causing local crushing of concrete, which is repairable (Figure 5.7).



Figure 5.6. Overview of precast industrial building connection damage in Kahramanmaraş



Figure 5.7. Corbel damages in Gaziantep

5. 1. 4. Performance of Non-Structural Elements

One of the most important non-structural damage in the region was observed in the infill walls. Several levels of damage events were observed depending on the strong ground motion levels (Figure 5.8). At low ground motion levels (<0.1 g), the infill wall-column/beam interfaces cracked. At moderate levels, the infill walls sustained inclined cracks with varying widths (0.5-2 mm).



Under such damage, despite the absence of any structural damage, the occupants safely left the building and were reluctant to occupy the building after the earthquake. Similar to our past observations after 2011 Van earthquake, the infill walls are observed to be the key components to establish the damage state of a building affecting the psychology of the occupants. The infill wall construction technique suggested in the latest seismic code in 2019 did not seem to be applied in any of the recent buildings. For regions that have experienced accelerations well over the design values, the infill walls were severely damaged and failed under combined in and out of plane. Infill wall damage was observed in buildings constructed both before and after year 2002 exhibiting no significant difference in their performance. Furthermore, the damage was similar in all the infill walls made of hollow clay brick, autoclaved aerated concrete or bims blocks, indicating that none of the block materials showed superior seismic performance.



Figure 5.8. Infill wall damage examples

5. 1. 5. Performance of Masonry Buildings

Masonry construction constitutes the second largest type in Turkish building inventory. Although the percentage of masonry buildings in urban areas is low, it is more common in rural areas. Similar to the other buildings, non-engineered masonry building stock in the region either suffered significant damage or collapsed under the two earthquake motions (Figure 5.9). However, the collapse of masonry buildings constructed with relatively better materials having 1-3 stories was less compared to 8-10 story RC buildings. It appears that the height and rigidity of the buildings played an important role. Besides, many historical masonry buildings suffered heavy damage or collapse due to strong shakings that they experienced.



Figure 5.9. Damage in masonry structures

5. 1. 6. Performance of Strengthened Buildings

One building strengthened in 2008 by the METU team with the addition of shear walls, fiber reinforced polymers was visited in Hatay. None of the strengthened buildings collapsed while some damage was observed, as shown in Figure 5.10. These observations that will be extended in further site visits seem to encourage the wider spread application of building strengthening.



Figure 5.10. Performance of the strengthened building in Hatay

5. 1. 7. Performance of Electrical Substation Buildings

Service buildings (typically 1-2 stories) in twenty-three substations were visited to check the damage levels. The locations of the substations are shown in Figure 5.11. It can be observed that some of the substations are located in close proximity to strong ground shaking. However, none of the switch yard or control buildings were heavily damaged to disrupt the operation of the substations. It can be stated that the successful building performance of the substation buildings allowed continuous electricity transmission in the earthquake region.

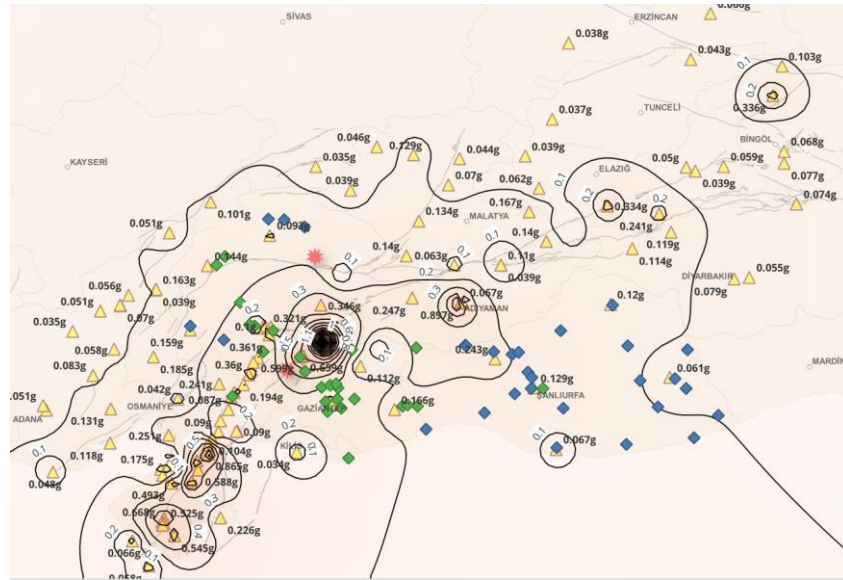


Figure 5.11. PGA distribution and substation locations (Yellow: Strong motion instruments, Blue and Green: Substation Locations)



Chapter 6.

Performance of Bridges and Tunnels

By:

Alp Caner^(a), Kemal Önder Çetin^(a), Candan Gökçeoğlu^(b)

(a) Middle East Technical University, Civil Engineering Department, Ankara, Türkiye

(b) Hacettepe University, Geological Engineering Department, Ankara, Türkiye



6. 1. Bridge and Tunnel Condition Assessment

In the successive major earthquakes, no collapse or loss of lives was observed or reported associated with poor bridge and tunnel performances. In the disaster region, there are more than 1000 bridges. Only 15 bridges were affected by these events, and about 50% were opened to traffic within a day after the shakings. One railway tunnel, near Ozan village, Gölbaşı was severely damaged by the earthquakes. This tunnel was constructed in the 1940s, and it is a stone-lining tunnel. Except this tunnel, the remaining tunnels performed well with some minor damages. Linings experienced some concrete spalling, and some minor portal damages were observed.

More specifically, no serious damages were observed in the tunnels constructed in the last three decades. The Nurdağı Portal of the Bahçe-Nurdağı Tunnel twin tunnels, the longest railway tunnels of Türkiye with a length of approximately 10 km, is near the active fault. The portals and the segments experienced no damage. However, some rockfalls were observed in the Nurdağı Portal of this tunnel. Additionally, the Tarsus-Gaziantep Motorway Tunnels between Bahçe and Nurdağı showed a good performance. Visible signs of damage were not observed, and they were open to traffic. It can always be expected that damaged structures in the region may collapse under subsequent earthquakes in the future. For example, it has been observed several times that some of the damaged structures after the first earthquake collapsed in the second earthquake

The typical observed engineering problems are:

- Bearing and joints movements
- Expansion joint movements
- Abutment approach fill settlement
- Pounding at expansion joints
- Shear key damage
- Soil liquefaction
- Column concrete spalling and start of plastic hinges

Examples of bridges and tunnels can be seen in the following figures.



Figure 6.1. Abutment rotation due to seismic soil liquefaction induced foundation failure



Figure 6.2. Joint movements



Figure 6.3. Concrete spalling

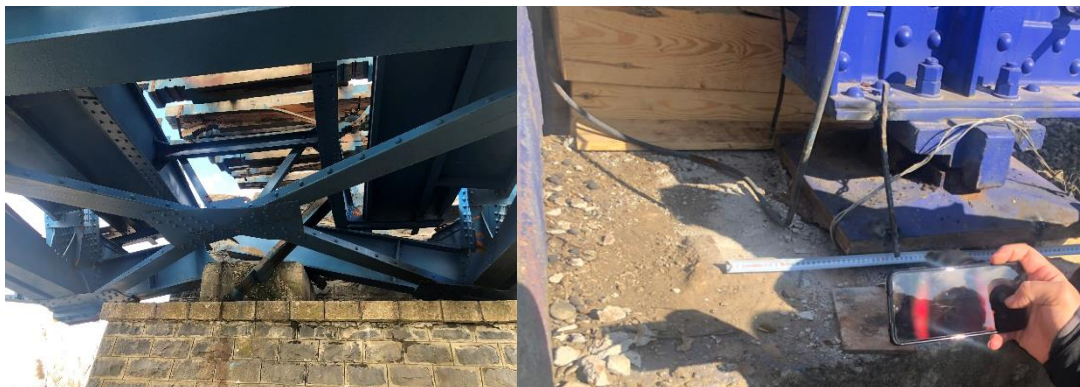


Figure 6.4. Bearing dislocation and movement



Figure 6.5. Rail misalignment



Figure 6.6. Shear key damage



Figure 6.7. Abutment wall concrete spalling



Figure 6.8. Bridge typical have no damage



Figure 6.9. Tunnel portal movement and concrete spalling



Figure 6.10. Nurdağı portal of Bahçe-Nurdağı railway tunnels



Chapter 7.

Coastal Structures in the Gulf of İskenderun and Tsunami in The Eastern Mediterranean

By:

Ahmet Cevdet Yalçınmer^(a), Gözde Güney Doğan^(a), Işıkhan Güler^(a), Bilge Karakütük^(a),
Furkan Demir^(a), Didem Cambaz^(b), Vassilios Skanavis^(c), Costas Synolakis^(c,d)

- (a) Middle East Technical University, Ocean Engineering Research Center, Ankara, Türkiye
- (b) Boğaziçi University, Kandilli Observatory and Earthquake Research Institute, İstanbul, Türkiye
- (c) Academy of Athens, Greece
- (d) University of Southern California, USA



7. 1. Coastal Structures in the Gulf of İskenderun and Tsunami in The Eastern

Mediterranean

After the 06 February 2023 01:17 (UTC) event, as the Tsunami Service Provider, KOERI issued four tsunami messages with a tsunami warning 15 min (after the earthquake) with expected tsunami amplitudes above 0.5 m along the southern coast of Türkiye. As one of the UNESCO IOC NEAMTWS (UNESCO, Intergovernmental Oceanographic Commission, Northeast Atlantic, Mediterranean, and the connected seas Tsunami Warning System) Tsunami Service Provider, Boğaziçi University Kandilli Observatory and Earthquake Research Institute (KOERI) issued four tsunami messages according to the decision matrix based on earthquake magnitude and location, with a tsunami warning 15 min (after the earthquake) with expected tsunami amplitudes above 0.5 m along the southern coast of Türkiye. Although the epicenter is ~90 km inland, the earthquake generated a tsunami, which is measured at four tide gauge stations, (İskenderun-Arsuz, Erdemli, Gazimagusa (Famagusta), and Girne (Kerinya) in the Eastern Mediterranean. The recorded water motions have been analyzed after deciding to distinguish the arrival time of the wave and the profile of the water level fluctuations. The tide gauge record in Arsuz shows a ~14 cm positive and ~10 cm negative tsunami amplitude with approximately a 10 min wave period. The arrival times of the first and maximum waves are around 25 min and 33 min after the earthquake, respectively. The first wave arrivals are around 36 min at Gazimagusa (Famagusta) and 48 min at Erdemli and Girne (Kerinya) stations. The maximum tsunami amplitudes are measured as 13 cm at Erdemli (54 min), and 17 cm at Gazimagusa (Famagusta) (65 min).

Although the tsunami event is small-scale, scientific investigation and understanding of the source location and the generation mechanism are important for possible future tsunami events and preparedness. The tsunami has also been a test for the effective working and communication of the early warning system in the area. For the assessment of the 6 February 2023 small amplitude tsunami, numerical simulations are performed using the tsunami numerical model NAMI DANCE. For topography and bathymetry EMODnet (<https://emodnet.ec.europa.eu/en/bathymetry>, ~105 m resolution) and ASTER (<https://asterweb.jpl.nasa.gov/gdem.asp>, ~30 m resolution) data are used. The modeling database is established as a 100 m grid size covering the Eastern Mediterranean. The arrival times of the waves at the four tide gauges indicate a possible tsunami origin North of Samandağ near Kale cape with a source of bipolar elliptical subsidence and uplift shape (Figure



7.1 (a). Mass movements are possible atypical (nonseismic) tsunami sources but those hypotheses regarding this event need more data and further analysis. The distribution of the maximum water elevations computed by 120-minute simulations of the possible source considered in the North of Çevlik is given in Figure 7.1 (b).

The February 6, 2023, tsunami needs to be well understood in terms of the source areas and generation mechanisms. A field survey is performed on February 11-13, 2023, to investigate the tsunami traces, conduct eyewitness interviews, identify the types and locations of the possible sources, and investigate the damage to the coastal structures. The field survey covered the coast of the Gulf of Iskenderun from Karatas (West) to Samandağ-Çevlik (East).

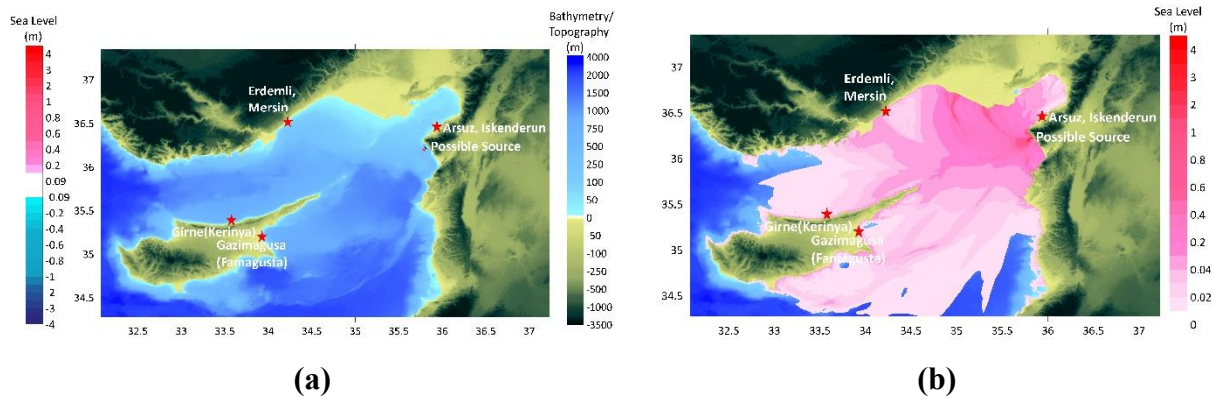


Figure 7.1 a) The location of the possible source of small amplitude tsunami and the tide gauge stations, and **b)** distribution of maximum water elevations computed from the possible source, North of Çevlik

Simulations are performed using the survey findings and the numerical results are compared with the tide gauge measurements. Figure 7.2 shows the comparison of the measured (black) and computed (blue) time histories at four tide gauge stations. The additional time histories of modeling results are presented for the localities near Karataş, Yumurtalık, and Çevlik fishery ports, where the eyewitness observations are collected from the fishermen or coast guard staff. The arrival times of the first wave nearly fit with the measured data. However, more detailed modeling studies are required to determine the location and type of the source when new data is collected by new field studies.

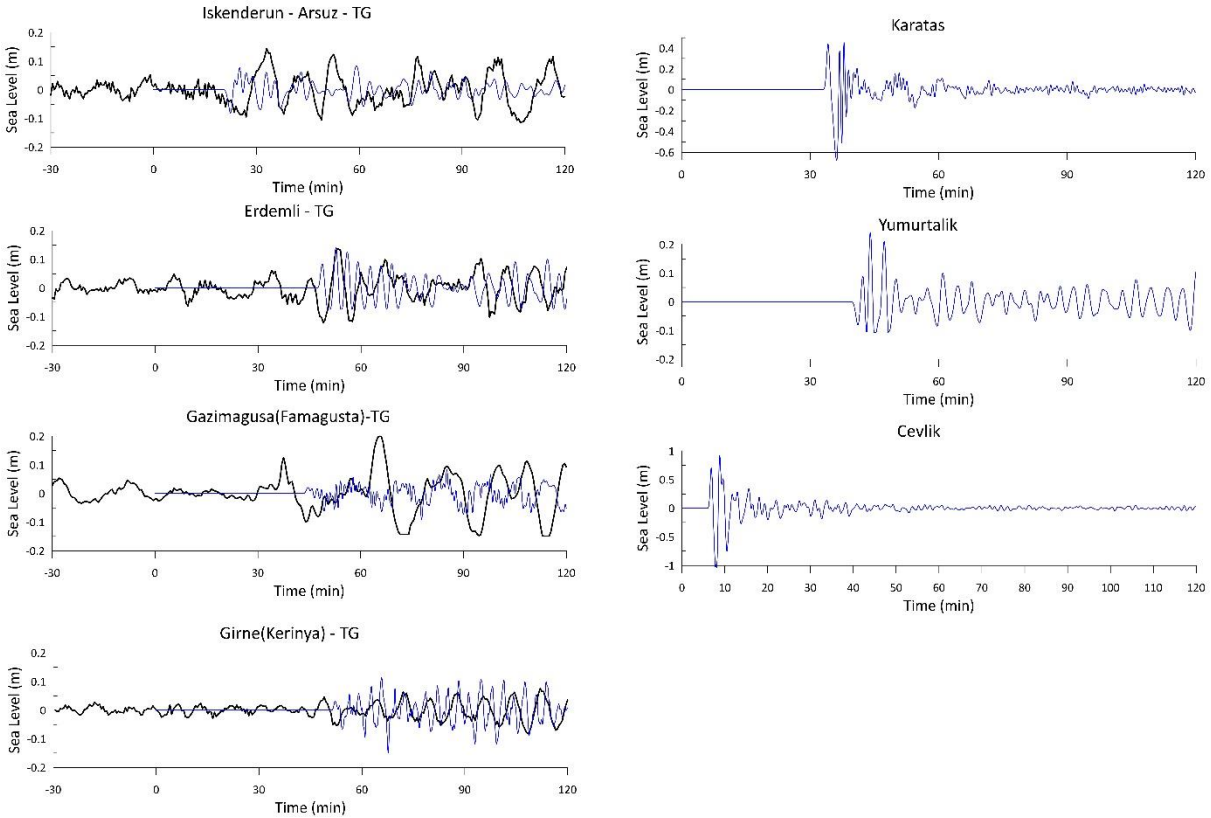


Figure 7.2 The comparison of the measured (black) and computed (blue) time histories of water surface fluctuations at four tide gauge stations (first column) and computed time histories near Karataş, Yumurtalık and Çevlik fishery ports, where only eyewitness observations (second column) could be obtained.

Some of the pictures taken during the field survey are also presented in Figures 7.3 and 7.4. Figure 7.3 shows the traces of the coastal inundation observed in the morning after the earthquake near the Samandağ fishery port at Çevlik village. Figure 7.4 shows the damages to the coastal structure and the pier of İskenderun fishery port, which are the results of the coastal subsidence at the reclamation area, backside of the fishery port, and nearby coastal region.



Figure 7.3 Coastal Inundation and traces, South of Samandağ-Çevlik Fishery Port



Figure 7.4 Structural damage at İskenderun Fishery Port

Days after the earthquake, considerable water inundation has been observed behind and on the eastern side of the İskenderun Fishery port, which has drawn the attention of the general public to consider the tsunami as a reason. However, the observations and evidence obtained during the field survey clearly identified that the reason was the subsidence of the coastal area behind the fishery port during the earthquake shaking most probably due to the liquefaction or similar means. During high tide (because of full moon days), seawater gradually invaded the subsided area and could not be drained because of collapsed surface water drainage system. Therefore, the phenomenon that



occurred in the area is the gradual invasion of seawater by the high tide during the full moon phase to the area, where the ground subsided considerably.

The report will be updated with new data from the field and with new simulations using a higher-resolution database and other possible source alternatives.

Acknowledgments: This study is supported by TUBITAK 1002 C Quick Support Grant, METU, Bogazici University and European Commission European Civil Protection and Humanitarian Aid Operations DG-ECHO funded UNESCO-CoastWAVE Project. Headquarter of General Command of Turkish Coast Guard and commanders of Coast Guard in the bases of Iskenderun Bay facilitated the survey significantly. Zülfikar İnönü Tümer, Saffet Aslan, Erdiñç Altıok, Emin Bilen Tümer are acknowledged for their valuable support and logistics. Semih Taş, Ömür Küçükkör and Mustafa Ünlü are also acknowledged for their collaboration and valuable eyewitness information.



Chapter 8.

Preliminary Reconnaissance Observations on Lifelines After 6 February 2023 Earthquakes in Türkiye

By:

Nejan Huvaj^(a), Volkan Kalpakçı^(b), Şevki Öztürk^(c), Tamer Y. Duman^(d), Eray Baran^(a),
Burak Talha Kılıç^(a), Ali Serdar Uysal^(d), Suat Dalkılıç^(e), Emre Dalkılıç^(e), Onur Pekcan^(a)

- (a) Middle East Technical University, Civil Engineering Department, Ankara, Türkiye
- (b) GEOCE, Ankara, Türkiye
- (c) Çankaya University, Civil Engineering Department, Ankara, Türkiye
- (d) Fugro Sial, Ankara, Türkiye
- (e) EMAD Enerji Harita, Ankara, Türkiye



8. 1. Introduction

Lifelines provide flow of resources and services that sustain communities and they are typically composed of linear, connected networks such as transportation corridors (highways, roads, railways, tunnels), water distribution pipelines, electric power transmission systems, gas and liquid fuel, communication networks/systems as well as other critical infrastructure such as airports, ports, and harbors. Lifeline systems have different, and perhaps more complex, vulnerabilities to earthquakes as compared to individual buildings and industrial structures. Disruptions in lifelines can lead to regional, national social, and economic impacts. Lifelines are constructed over broad geographical areas and they are interdependent, i.e. the disruption of one lifeline system may affect the performance of another. For example, water pumping stations or equipment control in liquid fuel and natural gas pipeline systems may use the energy provided by electric power networks. When multiple different lifelines gather or pass through the same area, all are vulnerable to disruption from a single cause, such as an earthquake.

In this section, we briefly describe the preliminary observations on the performance of lifeline system infrastructure in the region after the 6 February 2023 earthquakes in Türkiye. The preliminary fieldwork was conducted on 10-12 February 2023 (during 13-14 February 2023 some members of the team continued the field survey) in Kahramanmaraş and Gaziantep by a team composed of Nejan Huvaj, Volkan Kalpakçı, Şevki Öztürk, Eray Baran, Tamer Y. Duman, Burak Talha Kılıç, Ali Serdar Uysal, Suat Dalkılıç, and Emre Dalkılıç. We would like to acknowledge the funding provided for the fieldwork by The Scientific and Technological Research Institution of Turkey (TÜBİTAK) “1002-C Natural Disasters-Focused Fieldwork Emergency Support Program (Doğal Afetler Odaklı Saha Çalışması Acil Destek Programı)”. The preliminary objective of the reconnaissance efforts was to document the effects of the earthquakes on lifelines including the performances of railway systems, highways, water and gas pipelines as well as electric transmission systems, and to collect and document perishable data.

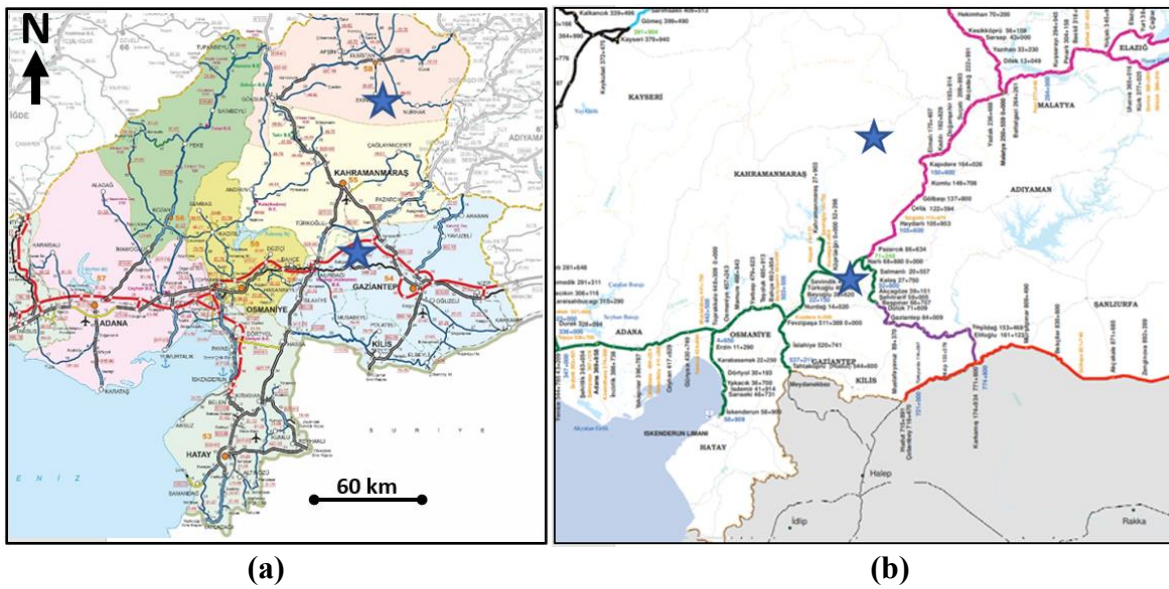
8. 2. Brief Information about the Critical Infrastructure in The Region

The lifelines in the study area support eleven cities with a total population of 14,013,196 people, constituting 16.4% of the 2022 population of Türkiye, which is 85,279,553 (data from Turkish Statistical Institute, <https://data.tuik.gov.tr/Bulten/Index?p=Adrese-Dayali-Nufus-Kayit-Sistemi->



Sonuclari-2022-49685, accessed on 17.02.2023). Some of the biggest cities (in terms of their 2022 population) that are significantly impacted by the earthquakes in the region are: Adana 2,274,106 population; Gaziantep 2,154,051; Hatay 1,686,043, Kahramanmaraş 1,177,436; Adıyaman 635,169; Malatya 812,580.

In order to demonstrate the size and distribution of the lifeline networks in the region, few examples of critical infrastructure maps (highways and railways) are provided (Figure 1). State Highway Agency, KGM, and State Railway Agency (TCDD) are the national authorities responsible for highways and railways, respectively. These maps, when considered together with their proximity to the epicenters of both earthquakes (approximately placed as star symbols in Figure 1), as well as the active fault lines in the region, can help visualize the scale of the possible impact on the lifelines over a large geographic area.



F
i
g
u
r

As for the state of damage and serviceability of the airports, railways and roads as well as gas and electricity services in the region after the two earthquakes, the information from National Disaster Agency (AFAD), provided on 06.02.2023, at 15:35 local time (few hours after the 2nd earthquake), published at The Press Bulletin No. 6. (<https://www.afad.gov.tr/kahramanmaraş-pazarcikta-1>)

1 a) Parts of the state highway network in the region (source: State Highway Agency, KGM website: <https://www.kgm.gov.tr/SiteCollectionImages/KGMimages/Haritalar/b5.jpg>), **b)** Parts of the state railway network in the region (source: Turkish State Railway Agency website: <https://static.tcdd.gov.tr/webfiles/userfiles/files/genel/tcddharita.pdf>)



[meydana-gelen-deprem-hk-basin-bulteni6](#)) noted that Kahramanmaraş, Gaziantep, Hatay airports were closed to operation due to damages caused by the earthquakes and electricity could not be provided to 27 communities/neighborhoods in the region (including Kahramanmaraş city, Osmaniye Bahçe-Düziçi, and some parts of Malatya city) due to earthquake-caused damages. Emergency repair works were carried out and alternative electricity resources were put into service and electricity was provided to Kahramanmaraş city within twenty-four hours after the 1st earthquake. As time went by, further checks were carried out by relevant state and local agencies and updates were given by AFAD on the state of lifelines. Information from National Disaster Agency (AFAD), on 07.02.2023, at 12:10 local time, published at The Press Bulletin No.10 of AFAD (<https://www.afad.gov.tr/kahramanmaras-pazarcikta-meydana-gelen-deprem-hk-basin-bulteni10>) noted that Kahramanmaraş and Hatay airports were closed to service due to damages caused by the earthquakes; Gaziantep and Şanlıurfa airports were open to aid flights; and Malatya, Adana, Diyarbakır, Adıyaman airports were open to service. Railway service through Fevzipaşa-Narlı, Narlı-Gaziantep, Narlı-Malatya railway lines were closed to service; Malatya-Çetinkaya, Malatya-Yolçatı railway lines were open to emergency use, and Ulukışla-Adana, Adana-Mersin, Adana-Toprakkale, Yolçatı-Diyarbakır, Yolçatı-Elazığ, Elazığ-Tatvan railway lines were open to rail traffic. In terms of roads, Adıyaman-Çelikhan road, Osmaniye-Gaziantep direction, Hatay-Reyhanlı state highway, Hatay Kırıkhan-Topboğaz roads were closed to traffic; Adıyaman-Çelikhan-Sürgü Road Balık Burnu bridge has collapsed; Adıyaman Gölbaşı-Malatya Sürgü road was closed due to landslides and Şanlıurfa-Gaziantep road was open to traffic. Soon after, emergency repair and recovery operations were carried out by all relevant state agencies.

BOTAŞ Petroleum Pipeline Corporation is the state-owned crude oil and natural gas pipelines and trading company in Türkiye, which provides natural gas service in the region. TEİAŞ, Turkish Electricity Transmission Corporation, a government-owned corporation, is the transmission system operator for electricity in Türkiye. According to the State National Television TRT's press quotes of the Ministry of Energy and Natural Resources of Türkiye, Mr. Fatih Dönmez, published on 06.02.2023, there were some damages and disruptions in the electricity and natural gas infrastructure on the day of the earthquakes (<https://www.trthaber.com/haber/gundem/bakan-donmez-deprem-bolgesinde-enerji-hatlarinda-hasarlar-var-743813.html>, accessed on 17.02.2023), however, immediate repair efforts and utilization of alternative solutions helped a



quick recovery in the infrastructure system. For example, electricity was brought to the city of Kahramanmaraş within 24 hours of the first earthquake.

One of the significant damages was observed in the main natural gas transmission line, in Türkoğlu county, which is located near the epicenter of the one of the earthquakes, and serves the cities of Kahramanmaraş, Gaziantep, Hatay according to the Ministry of Energy's TRT news quote. According to the Information Note released by BOTAŞ, the gas supply was remotely cut-off right after the earthquakes. Critical facilities in the region were immediately supplied with CNG and LNG while repair works were ongoing. According to the press quotes of the Ministry of Energy and Natural Resources of Türkiye published on 11.02.2023, this natural gas transmission line was repaired and put back into service on 11.02.2023 (<https://www.dunya.com/gundem/bakan-donmez-acikladi-deprem-bolgesindeki-evlere-elektrik-verilecek-mi-haberi-685515>, accessed on 17.02.2023). However, in areas where building damages were significant, gas supply is not connected to buildings unless the building safety level and the safety of the gas transmission system are confirmed. Finally, as part of precautionary measures, controls on the pipelines designed according to ASME Standart B31.8 continue uninterruptedly in the fault approach regions or inevitable crossings due to the faults.

8. 3. Field Observations on Lifelines

The region has been particularly affected by ground rupturing (left-lateral slip motion) of the faults and intense seismic shaking, demonstrated by typically observed damages such as:

- Surface fault rupture-induced deformations, offset, buckling, uplift and subsidence on asphalt roads, highways, railway tracks as well as on unpaved roads and farmlands
- Landslides and rockfalls triggered by the earthquakes disrupting the road and railway networks
- Ground deformation-triggered damage and partial disruption of the water pipeline systems
- Cracks, tilt, lateral displacement and damages on retaining walls
- Damages caused by ground deformations on airport pavements and access roads
- Tilt and damages on electric poles, buried utilities, broken underground pipelines

Examples of such damages can be seen in the following figures.

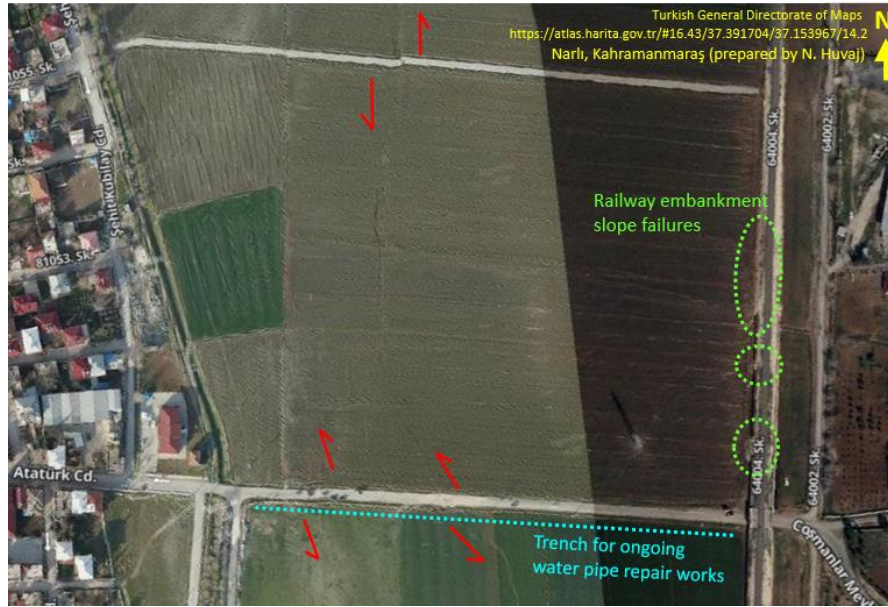


Figure 8.2. Areal view of the surface fault rupture and examples of damages caused by the two earthquakes on some of the lifelines: railway line, roads and water distribution network, near Narlı, Kahramanmaraş (Satellite images are provided by Turkish General Directorate of Maps via atlas.harita.gov.tr website)

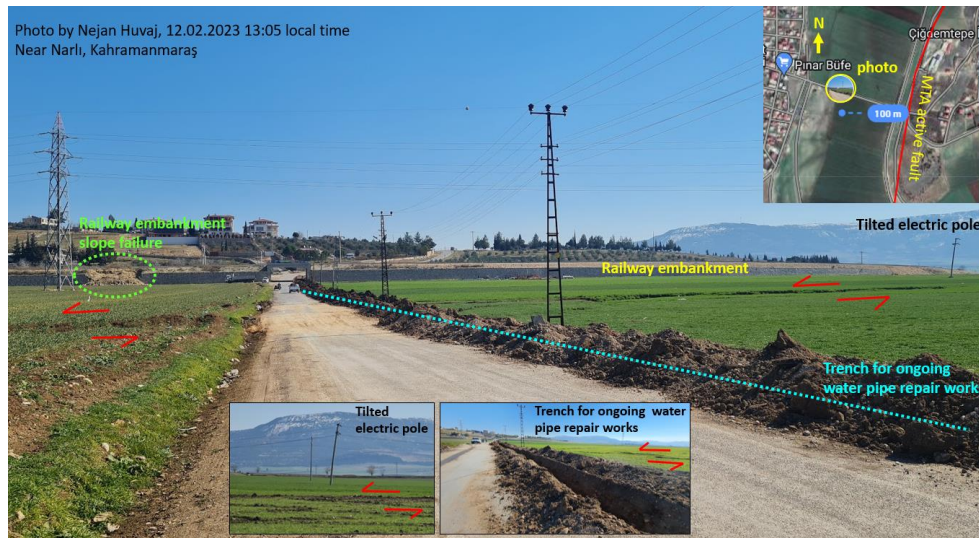


Figure 8.3. Referring to Figure 2 for locations of the photos: offset on the road due to surface fault rupture, railway embankment slope instability, water pipeline repair works and a tilted electric pole can be seen, near Narlı, Kahramanmaraş. (Active fault data is taken from Emre et al. (2013) published by the General Directorate of Mineral Research and Exploration, MTA (Maden Tetkik ve Arama Genel Müdürlüğü)).



Figure 8.4. Surface rupture, offset, cracks and damages on railway tracks and roads, as well as a damaged electric tower, near the surface rupture (Narlı, Kahramanmaraş). (Active fault data is taken from Emre et al. (2013)).



Figure 8.5. A landslide and crack/damages on the road next to a water canal, causing significant lateral displacement of a concrete retaining wall (pushed towards the water canal), a tilt on an electric pole, in southern part of the city of Kahramanmaraş (active fault data from Emre et al. (2013)).



Figure 8.6. Surface rupture observations causing a 3.6 m offset on Gaziantep-Kahramanmaraş road, cracks on the asphalt road at several locations, road embankment instability and more than 250 m-long longitudinal cracks at the top of the road embankment as well as on the asphalt road, near Kıpıçam, Kahramanmaraş (Satellite images are provided by Turkish General Directorate of Maps via atlas.harita.gov.tr website)



Figure 8.7. Referring to Figure 6 for the location: surface rupture observations and 3.6 m offset on Gaziantep-Kahramanmaraş road (active fault data from Emre et al. (2013)).



Figure 8.8. Landslides and surface cracks on the roads, near Kartal and Yarbaşı, Kahramanmaraş (Active fault data from Emre et al. (2013)).



Figure 8.9. Landslides, rockfalls and surface cracks on the roads, near Fevzipaşa, Gaziantep causing disruption in the service (Active fault data from Emre et al. (2013)).



Acknowledgments: We would like to acknowledge the funding provided for the fieldwork by The Scientific and Technological Research Institution of Turkey (TÜBİTAK) “1002-C Natural Disasters-Focused Fieldwork Emergency Support Program (Doğal Afetler Odaklı Saha Çalışması Acil Destek Programı)”.

References:

Emre, Ö., Duman, T.Y., Özalp, S., Elmacı, H., Olgun, Ş. ve Şaroğlu, F., 2013, Açıklamalı Türkiye Diri Fay Haritası. Ölçek 1:1.250.000, Maden Tetkik ve Arama Genel Müdürlüğü, Özel Yayın Serisi-30, Ankara-Türkiye. ISBN: 978-605-5310-56-1), published by the General Directorate of Mineral Research and Exploration, MTA (Maden Tetkik ve Arama Genel Müdürlüğü).

ASME Standart B31.8 (Gas Transmission and Distribution Piping Systems)



Chapter 9.

Preliminary Structural Performance Summary of Historic Structures

By:
Ahmet Türer^(a)

(a) Middle East Technical University, Department of Civil Engineering, Ankara, Türkiye



9. 1. Introduction

Structural evaluation of historic structures which are part of architectural heritage in Türkiye is important with regards to i) restoration maintenance related issues from conservation of architectural heritage point of view and ii) earthquake performance of historic masonry structures as a part of civil engineering practice. A site visit to Malatya and Elazığ cities was carried out as a team effort together with T.R. Directorate General of Foundations - Republic of Türkiye Ministry of Culture and Tourism. Some of the mosques and mausoleums were visited after the earthquake; this chapter summarizes the preliminary performance evaluation of visited sites (historic mosques, minarets, and mausoleums) as well as gathered information on Gaziantep Castle and a church performance from Hatay.

9. 2. Visual Inspection of the Historic Structures

Southeastern Türkiye has a rich cultural heritage structure stock that is in the form of houses, bridges, earliest churches, synagogues, mosques, castles, and listed UNESCO World Heritage Sites (**Figure 9.1**)¹. The eleven cities that are affected by the recent earthquakes (**Figure 9.2**)² are listed as Kahramanmaraş (520), Gaziantep (906), Malatya (685), Diyarbakır (1113), Kilis (420), Şanlıurfa (1764), Adıyaman (144), Hatay (1099), Osmaniye (161), Adana (874), Elazığ (301)³ and contains about 8 thousand registered cultural heritage. Malatya and Elazığ cities were selected for evaluation of historic structures since cities closer to the epicenter were more difficult to access since the survivor rescue missions were given the priority. About a dozen structures in Malatya and about 20 sites in Elazığ were visually investigated on site. Additional few historic structures were also evaluated based on visual information obtained from the internet using satellite imaging and photos on the news. These are the Gaziantep Castle, Antakya Rum Orthodox Church, and Antakya Protestant Church. Damage patterns are investigated and briefly reported.

¹ <https://globalheritagefund.org/places/mena/>

² https://www.google.com/maps/@37.4892096,35.1985455,7z/data=!4m2!2m1!1s%2Fg%2F11shww_tpt

³ Republic of Türkiye Ministry of Culture and Tourism data, gathered by Assoc. Prof. Dr. Nurdan Kuban, Kocaeli Univ.



9

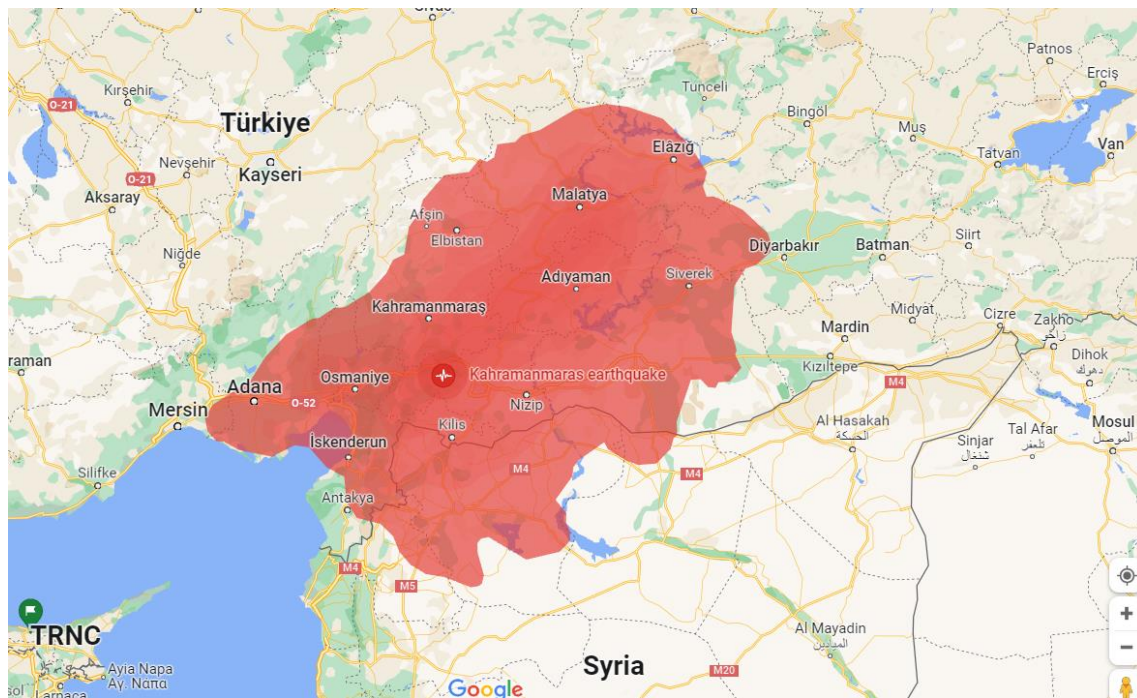


Figure 9.2 Cities affected by the Kahramanmaraş earthquakes including Malatya and Elazığ.



The first earthquake's epicenter distance to Malatya and Elazığ cities is about 165 km and 250 km, respectively; while, the second earthquake epicenter to Malatya and Elazığ is about 100 km and 190 km, respectively (**Figure 9.3**) and has been more damaging for these two cities than the first one. Malatya being about half distance closer to both earthquakes with respect to Elazığ, the damage is expected to be larger in Malatya. Most devastating damage was observed at central Malatya, a relatively large mosque with the name Yeni Cami (new mosque, about 100 years old) suffered significant damage and major collapse. Before and after earthquake pictures (**Figure 9.4**) of Yeni Cami show the level of damage; which raised concerns since the mosque was recently renovated and strengthened. Although a thorough investigation is necessary before any conclusions can be drawn, the collapsed newly added buttress and insufficient anchorage to the existing walls seem to be one of the factors that went wrong.

Other historic structures in Malatya region were investigated in the Eski (old) Malatya part of the city, which resided most of the historic structures. About 12 mosques and mausoleums were observed in this area with minor to medium damage, but total collapse was not observed. The common damage and failure types may be listed as:

- a) Minaret top cracked and slightly moved,
- b) Minaret body had a horizontal crack towards the bottom but remained in position,
- c) Perpendicular wall connection had a slight crack which is minor and may be fixed with paint,
- d) Vaults were cracked at the top crest indicating compression levels exceeding material capacity,
- e) Some newly constructed buttresses failed because of insufficient anchorage length and lack of interlocking between wall and buttress stones.

In addition to these mentioned damage mechanisms, some of the walls have been noticed to crack diagonally and compression failure by dislocated stones and cracking at the mortar level were observed. However, only one mosque had total collapse (relatively new and stone masonry), but older historic structures have proved to be worthy to survive centuries and still in good condition.

The historic structures in Elazığ region showed lesser amount of structural damage from the recent earthquakes. Minor cracking (if any) in the historic masonry mosques and masonry buildings such as hamam (Turkish bath) indicated that the buildings remained in linear elastic range. If properly



maintained and water damage is prevented, the historic structures have proven themselves to survive centuries without any significant earthquake damage. It was observed that tension rods were added in some of the smaller mosques at the arch level and may have some positive impact on the overall earthquake performance of masonry buildings, which are sturdy in general with relatively small rooms and thick walls. Two reinforced concrete mosques in Elazığ city had minor cracks in the 2020 Elazığ Earthquake and the same cracks remained intact with small amount of cement dust on the carpets but no major or minor damage. Corners of the mosques that suffered humidity from the roof had also some flakes on the ground, which was told to be a regular cleaning task with or without earthquakes.



Eski (old) Malatya

Harput



Figure 9.3 Geographic location of the historic structures evaluated in Malatya and Elazığ.



Figure 9.4 Yeni Cami (new mosque) before and after pictures and short anchorage.

An important historic heritage located in south eastern Türkiye is Gaziantep Castle (**Figure 9.5**). Unfortunately, Gaziantep to the epicenter of the first earthquake is only about 32 km and the second earthquake is about 115 km distance. The orientation of the castle walls to the earthquake epicenter



may be the reason for south-west castle walls to suffer the largest damage when the first impact must have pushed these walls and sending wall stones towards the slope towards the city. It is fortunate that the castle wall stones did not cause major damage to people, houses, businesses at the skirts of the castle. The castle being located at the top of a hill may also had lens action amplifying the pga and damaging effects of the earthquakes.



Figure 9.5 Gaziantep Castle before and after the earthquakes.



Last examples of historic structures were selected from Hatay region. The Antakya Rum Orthodox Church (Antioch Greek Orthodox Church) and Antakya Protestant Church are located very close to each other within 150 meters, and both suffered significant damage during the earthquakes. The distances between the churches and the first and second earthquakes are about 135 km and 225 km respectively. Satellite images before and after the earthquakes (**Figure 9.6.**)⁴ indicate that both structures suffered immense damage. The after-earthquake picture of the Antakya Rum Orthodox Church (**Figure 9.7.**) shows total roof collapse while only west wall and partial south cylindrical walls are standing. The collapsed picture of the Antakya Rum Orthodox Church also shows roof collapse with probably south wall collapse. The epicenter to the historic structures distances is comparable between Malatya and Hatay, both cities with significant damage to their historic buildings. Majority of the mosques showed acceptable performance in Malatya (exception of Yeni Cami) while both studied churches suffered major damage in Hatay.

The level of damage to historic structures depend on many parameters other than the distance to the epicenter as many times discussed here. Some of the other significant parameters controlling damage to historic structures may be listed as a) poor ground conditions, groundwater level, soil-structure interaction, foundation type and properties, earlier relative settlement of the structure, tilt of columns and walls, b) presence of tension-shear elements such as wooden lintels inside and corner of the walls and tension rings around the domes, c) discontinuous (before the edge wall) arches and vaults, d) buttresses that are not fully integrated with the wall, e) poor or weakened material and workmanship quality, frequency of maintenance of the structure and water damage – excessive moisture, f) interlocking mesh at walls connections and free (unsupported out of plane) spacing between orthogonal walls, g) past war, earthquakes damages; quality of repair and restorations; adding or removing sections from the walls, h) the symmetry of the building, i) the minaret being inside the wall or independent of the building, j) the bell towers and minarets being too slender and the whipping effect for the bell and minaret balcony, k) the presence of tension rods on the arches and vaults, their quality to column and wall connection, l) slenderness of walls and columns, m) spacing and dimensions of window and door openings in walls, minarets, and domes, n) ratio of wall thickness to height and unsupported length perpendicular to the plane, o) dimensions of cut stone, quality of rubble masonry, p) the match between the earthquake response

⁴ Google Earth images.



spectrum and the natural modal frequencies of the structure, q) the earthquake magnitude, the distance to the earthquake epicenter, the movement type of the fault, the presence of mountains that will reflect earthquake waves, r) the presence and quality (rusting and expansion) of horizontal and vertical locking metal braces between stones, s) the stair overlap ratios and the number of overlaps in a minaret, t) vertical joints between stones in a wall being aligned (not staggered), u) vandalism and treasure hunting etc should be mentioned. Existing historical building performance and damage observations have been made in the form of rapid preliminary assessment. Some of the structures that require a comprehensive examination must be re-evaluated with a closer and more detailed look considering most of the items listed above.

Acknowledgments: The author acknowledges kind help and collaboration received from the T.R. Directorate General of Foundations - Republic of Türkiye Ministry of Culture and Tourism regarding this work.



Figure 9.6 The Antakya Rum Orthodox and Protestant Churches before and after earthquakes



Figure 9.7 The Antakya Rum Orthodox Church after the earthquake ⁵

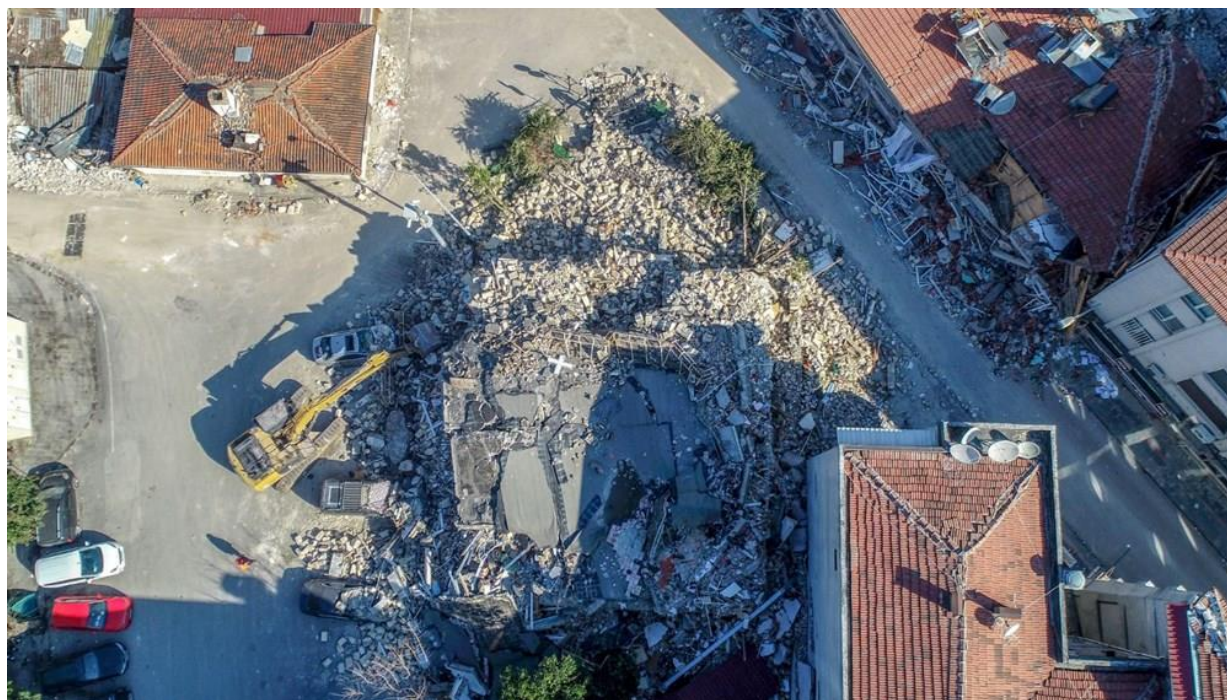


Figure 9.8 The Antakya Rum Protestant Church after the earthquake ⁶

⁵https://www.ntv.com.tr/galeri/turkiye/deprem-antakyadaki-tarihi-kiliseleri-yikti,MFWsAij73UqDkzS2avW3_A/XTLZYWkAQkKjGWjO0SLVCw

⁶ <https://haberortakoy.com/deprem-antakyadaki-tarihi-kiliseleri-yikti/>



Chapter 10.

Emergency Response and Community Impact

By:

Meltem Şenol Balaban^(a), Ali Fırat Çabalar^(b), A. Nuray Karancı^(c), Canay Doğulu^(d), Gözde İkizer^(e), Haldun Akoğlu^(f), Müge Akın^(g), Nil Akdede^(h), Onur Karakayalı⁽ⁱ⁾, Özlem Özdemir^(j), Sarper Yılmaz^(k), Selin Güzel^(l), Serkan Yılmaz^(m), Sıdıka Tekeli Yeşil⁽ⁿ⁾, Tolulope Ajobiewe^(o), Yeşim Ünal^(p) (in alphabetical order)

- (a) Middle East Technical University, Department of City and Regional Planning, Ankara, Türkiye
- (b) University of Gaziantep, Geotechnical Engineering, Gaziantep, Türkiye
- (c) TOBB University of Economics and Technology, Department of Psychology, Ankara, Türkiye
- (d) TED University, Department of Psychology, Ankara, Türkiye
- (e) TOBB University of Economics and Technology, Department of Psychology, Ankara, Türkiye
- (f) Marmara University, Faculty of Medicine, Department of Emergency Medicine, İstanbul, Türkiye
- (g) Abdullah Gül University, Department of Civil Engineering, Kayseri, Türkiye
- (h) Atılım University, Department of Architecture, Ankara, Türkiye
- (i) Sakarya University, Faculty of Medicine, Department of Emergency Medicine, Sakarya, Türkiye
- (j) Middle East Technical University, Department of Business Administration, Ankara, Türkiye
- (k) University of Health Sciences Dr Lutfi Kırdar Kartal Education and Research Hospital, Department of Emerging Medicine, İstanbul, Türkiye
- (l) Middle East Technical University, Graduate School of Natural and Applied Sciences, Geodetic and Geographic Information Technologies, Ankara, Türkiye
- (m) Kocaeli University, Faculty of Medicine, Department of Emergency Medicine, Kocaeli, Türkiye
- (n) Fraunarzt Praxis Rheinfelden, Rheinfelden, Switzerland
- (o) Middle East Technical University, Graduate School of Social Sciences, Urban Policy Planning and Local Governments, Ankara, Türkiye
- (p) Haliç University, Department of Psychology, İstanbul, Türkiye



10. 1. Introduction

The "Emergency Response and Community Impact" section of the reconnaissance report was prepared by evaluating the period from the first earthquakes on February 6 to February 14, based on daily or even hourly preliminary data collected across the region. When this report is published, many of the problems pointed out here in the days and hours after the earthquake might probably be solved for many parts of the region. The main purpose of this section of the report is to reveal the actual situation in the emergency response and the effects of this situation on the communities in the period that lasted for 9 days after the major destructive earthquakes. An expanded version of this section is available on the METU-EERC website.

10. 2. Emergency Response

The preliminary evaluations of the possible impacts show the extent of the damages across the affected area covering 10 cities, with a population of approximately 14 million people. Together with the Syrian population living in the devastated area, the total affected population reached 15.8 million (TÜİK, 2022. See table 10.1 in the extended report). According to Türkiye's Emergency Response Plan (TAMP) which has been activated by the Turkish authorities at central and provincial level, search and rescue teams have been deployed to the region. The Turkish President announced a 3-month state of emergency on February 7, for the 10 provinces affected by the earthquake. Additionally, a Level-4 emergency has been declared in the country – which essentially entails a call for international assistance, initially focused on search and rescue support.

10. 2. 1. Coordination

The extensive damages on highways, roads, air and seaports, railways, accessibility problems created difficulties in transferring supportive search and rescue groups from other parts of Türkiye as well as foreign countries. On February 13th, Minister of Interior declared that “the total number of AFAD staff is 7300. It is not possible to manage such a great disaster or any disaster in Türkiye with such a limited number of staff.” There are approximately 300 thousand employees in the field as a total number of people who work for immediate rescue and response activities as the Minister highlighted.



10. 2. 2. Immediate Rescue and Response

Immediate rescue and response teams tried to reach disaster-stricken region. However, time lags occurred due to reasons like accessibility. Another issue on the site of collapsed buildings was that the necessary equipment for rescue operations, cranes, and trucks were scarce. During night times electricity blackouts at early stages of the events slowed down the S&R activities. It can be observed that emergency services including search and rescue teams, subsistence and medical aid were provided to the disaster-stricken region within the first 24 hours but not for all cities and villages simultaneously. On the other hand, evacuation of earthquake survivors started after within 72 hours.

10. 2. 3. Infrastructure

At 10:00 am on February 6, according to the first information received from disaster energy sources, natural gas cannot be supplied to Hatay/Hassa and Kırıkhan regions. BOTAŞ crude oil has been stopped as a precaution. As another precautionary measure, gas is cut from the entrance natural gas power plants of Gaziantep Nurdağı and İslahiye districts. 27 centers cannot be supplied with electricity. With the freezing winter conditions in the affected area, for about 3 to 4 days heating options were not possible. Another critical infrastructure is potable water system. The disaster-stricken area has no water supply for drinking and cleaning purposes due to damages on lines of potable water infrastructure.

10. 2. 4. Health Services

Voluntary and assigned healthcare personnel could only start to provide support to the region at the end of the second day. By the third day, a total of 2,101 ambulances, 296 UMKE vehicles, 5 air ambulances, 7 helicopter ambulances, and 14,429 emergency health personnel, including local and dispatched teams, were serving in the disaster area. As of February 12, 2023, a total of 21,631 patients rescued from the rubble were transferred to cities outside the region, 1,174 by air vehicles, 20,130 by land ambulances, and 327 by sea vehicles. As of February 14, 2023, 105,505 earthquake victims were rescued from the rubble as injured, and the number of casualties was announced as 35,418. It was reported that the number of public and private search and rescue personnel working in the region was 35,249, and 9,456 of them were international aid teams' personnel.



10. 2. 5. Accommodation Response: Emergency and Temporary Shelter

By February 13, 2023, 41,791 buildings had collapsed in these 10 cities (T.C. Çevre, Şehircilik ve İklim Değişikliği Bakanlığı, 2023c). The following day, February 14, 2023, nearly 195,962 people had to abandon their residences and leave their hometowns temporarily or permanently (AFAD, 2023a). Besides sports halls, educational buildings, and other governmental buildings, dormitories had opened their doors to the earthquake victims with the capacity of 850,000 beds in 81 cities (AFAD, 2023b). The latest updates as of 13 February 2023 by AFAD (2023a) show that the number of established family tents reached 155,379.

10. 2. 6. Psychosocial Support

The Ministry of Family and Social Services dispatched psychosocial support personnel to affected provinces. The Ministry of National Education (MEB, 2023a) also announced a Psychosocial Support Action Plan on February 10th, 2023. On February 13th, 2023, the Turkish Red Crescent (2023) released a statement that 53 psychosocial support teams (including psychologists, psychological counselors, social workers, and guidance specialists) have begun providing psychological first aid to earthquake survivors. Over 5,000 mental health professionals volunteered to provide psychological support to survivors in affected provinces.

10. 3. Community Impact

The impact of the devastating earthquakes on the community following the first week can be addressed mainly with respect to emergency response in relation to various decisions and activities bearing on education, rescue and relief efforts, and communication. Overall, it can be said that the emergency response decisions and activities following the Kahramanmaraş earthquakes did not consider the psychosocial needs of the affected people in the region at a desired level and that this lack of consideration seemed to have worsened the negative impact of the earthquakes on the community.

10. 4. Overview of International Media Response

A number of criticisms was levied against the emergency response activities and efforts of the Turkish authorities in the wake of the earthquake. Some of the criticisms were curated from published news reports and articles by international news agencies such as the BBC, CNN, Aljazeera, and the Financial Times. For example, for the initial days after the earthquakes the



Austrian Forces Disaster Relief Unit reported that Austrian Army suspended rescue operations at some point due to an “increasingly difficult security situation”, they however declared to resume their work as soon as government officials deems the situation to be safe.

10.5. Conclusion

Emergency response activities as a part of relief activities and initial recovery services are covered in the detail in this section as much as the data available. It is worth mentioning that, in the days, weeks and months ahead, there will be enough time to observe and report immediate macroeconomic impact of the earthquake.

The temporal graph of the emergency medical staff and services that have been transferred to the region after the earthquakes together with the number of casualties and injuries, has been produced as follows.

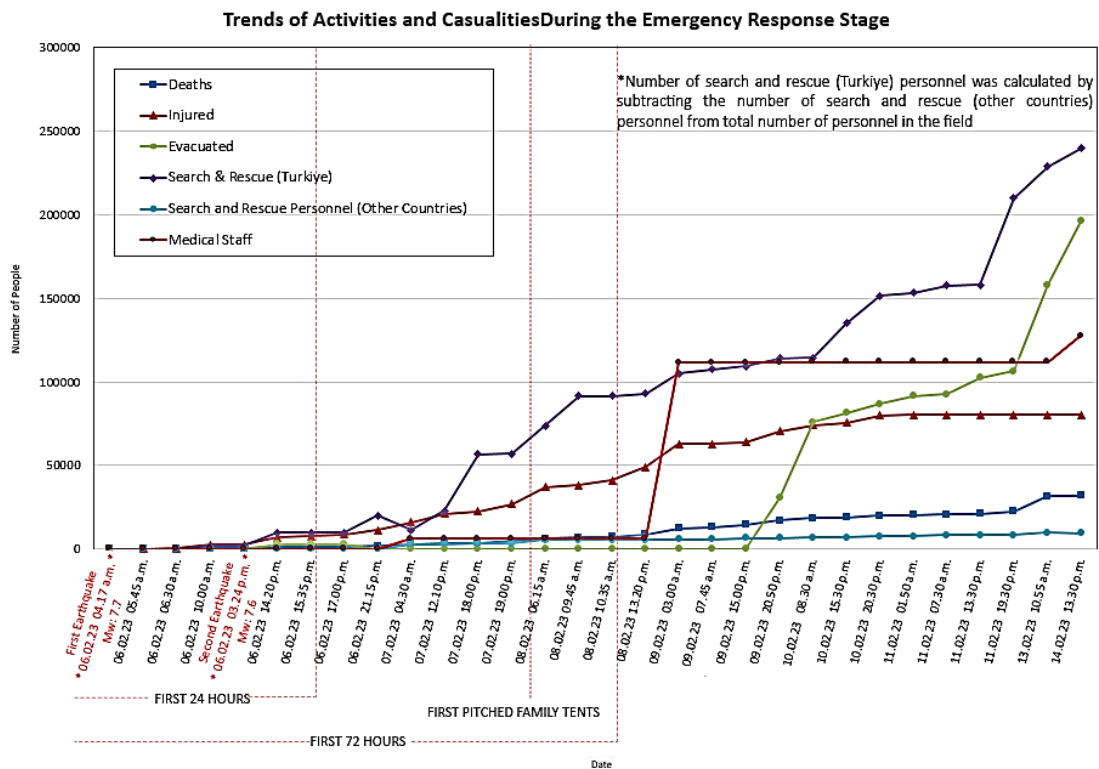


Figure 10.1. Map Trends of activities and casualties between February 6 to 14, 2023

Source: AFAD and Ministry of Health as of 14.02.2023 13:30 (GMT+3) (drawn by the authors)



References:

- AFAD. (2023a). *Duyurular*. T.C. İçişleri Bakanlığı Afet ve Acil Durum Yönetimi Başkanlığı. <https://www.afad.gov.tr/duyurular>
- AFAD. (2023b, February 6-14). AFAD. <https://twitter.com/AFADBaskanlik>
- AFAD. (2023c, February 13). *AFAD press bulletin about the earthquake in Kahramanmaraş - 28*. <https://en.afad.gov.tr/press-bulletin-28-about-the-earthquake-in-kahramanmaras>
- Anadolu Ajansı. (2023a, February 6). *Geçici Barınma Merkezleri*. Retrieved February 14, 2023, from <https://www.aa.com.tr/tr/info/infografik/32142>
- Anadolu Ajansı. (2023b, February 12). *Malatya'da 10 bin 500 kişilik konteyner kent kurulması için çalışmalar başladı*. Retrieved February 14, 2023, from <https://www.aa.com.tr/tr/asrin-felaketi/malatyada-10-bin-500-kisilik-konteyner-kent-kurulmasi-icin-calismalar-basladi/2816807>
- Railly News. (2023, February 7). *Psychosocial support personnel were dispatched to 10 provinces affected by the earthquake*. [https://www.raillynews.com/2023/02/Psychosocial-support-personnel-were-dispatched-to-10-provinces-affected-by-the-earthquake./](https://www.raillynews.com/2023/02/Psychosocial-support-personnel-were-dispatched-to-10-provinces-affected-by-the-earthquake/)
- Reuters. (2023, February 8). *Twitter restricted in Turkey two days after quake, says NetBlocks*. <https://www.reuters.com/business/media-telecom/twitter-restricted-turkey-netblocks-2023-02-08/>
- The Türkiye Emergency Response Plan (TAMP). (2022). Retrieved February 14, from https://www.afad.gov.tr/kurumlar/afad.gov.tr/e_Kutuphane/Planlar/TAMP.pdf#page=18&zoom=100,80,876
- T.C. Çevre, Şehircilik ve İklim Değişikliği Bakanlığı. (2023a, February 10). *Bakan Kurum: "10 ilimizde Cumhuriyet tarihinin en büyük afet konut seferberliğini başlatmış olacağız"*. Retrieved February 14, 2023, from <https://csb.gov.tr/bakan-kurum-10-ilimizde-cumhuriyet-tarihinin-en-buyuk-afet-konut-seferberligini-baslatmis-olacagiz-bakanlik-faaliyetleri-38419>
- T.C. Çevre, Şehircilik ve İklim Değişikliği Bakanlığı. (2023b, February 11). *Gaziantep'te 532 köyün tamamındaki depremzedelere yardım malzemesi gönderildi*. Retrieved February 14, 2023, from <https://www.csb.gov.tr/gaziantep-te-532-koyun-tamamindaki-depremzedelere-yardim-malzemesi-gonderildi-bakanlik-faaliyetleri-38421>
- T.C. Çevre, Şehircilik ve İklim Değişikliği Bakanlığı. (2023c, February 13). *Bakan Kurum: "10 ilde 41 bin 791 binanın yıkık, acil yıkılacak ve ağır hasarlı olduğunu tespit ettik"*. Retrieved



February 14, 2023, from <https://www.csb.gov.tr/bakan-kurum-10-ilde-41-bin-791-binanin-yikik-acil-yikilacak-ve-agir-hasarli-oldugunu-tespit-ettik-bakanlik-faaliyetleri-38426>

The Ministry of National Education [MEB]. (2023, February 10). *Psikososyal destek eylem planı ve psikososyal destek programları yayımlandı.* <https://www.meb.gov.tr/psikososyal-destek-eylem-planı-ve-psikososyal-destek-programları-yayımlandı/haber/29014/tr>

The Ministry of National Education [MEB]. (2023b, February 6). *Education is suspended until 13 February in Türkiye.* <https://www.meb.gov.tr/education-is-suspended-until-13-february-in-turkiye/haber/28950/en>

The Ministry of National Education [MEB]. (2023c, February 14). *Depremden etkilenen 10 ilde eğitim öğretime 1 Mart'a kadar ara verildi.* <https://www.meb.gov.tr/depremden-etkilenen-10-ilde-egitim-ogretime-1-marta-kadar-ara-verildi/haber/29029/tr>

Turkish Red Crescent. (2023, February 13). *Kızılay'ın psikososyal destek ekipleri deprem bölgesinde psikolojik ilk yardım veriyor.* <https://www.kizilay.org.tr/Haber/KurumsalHaberDetay/7202>

TURKSTAT. (2022). <https://www.tuik.gov.tr/>

Türk Mühendis ve Mimar Odaları Birliği [TMMOB]. (2023a, February 9). *TMMOB ön değerlendirme raporu yayımlandı.* <https://www.tmmob.org.tr/icerik/tmmob-degerlendirme-raporu-yayimlandi>

Türk Mühendis ve Mimar Odaları Birliği [TMMOB]. (2023b, February 14). *TMMOB Kahramanmaraş Depremi Güncel Durum Tespiti -2- (14 Şubat 2023).* <http://www.tmmob.org.tr/icerik/tmmob-kahramanmaras-depremi-guncel-durum-tespiti-2-14-subat-2023>

Türk Tabipleri Birliği. (2023, February 11). *6 şubat 2023 Depremi Bilgi Notu - 9: Geçici Barınma Yerlerinin şematik Yerleşim Biçimi.* Retrieved February 14, 2023, from https://www.ttb.org.tr/haber_goster.php?Guid=706d3bfa-aa11-11ed-b4b5-486b41055497

World Health Organization [WHO]. (2023, February 10). *WHO flash appeal: Earthquake response in Türkiye and whole of Syria.* https://cdn.who.int/media/docs/default-source/documents/emergencies/2023/who_flashappeal_earthquakeresponse_11-feb-2023.pdf?sfvrsn=94d4de2a_1